

Cite this: *Food Funct.*, 2025, **16**, 6080

# *Weizmannia coagulans* BC99 alleviates hyperuricemia by restoring liver–kidney–gut axis dysfunction caused by hyperuricemia†

Ying Wu,<sup>‡a,b</sup> Yinyin Gao,<sup>‡a</sup> Cheng Li,<sup>‡a</sup> Shirui Zhai,<sup>a</sup> Yao Dong,<sup>d</sup> Shanshan Tie,<sup>a,b</sup> Lina Zhao<sup>a,c</sup> and Shaobin Gu<sup>ID \*a,b,c</sup>

Hyperuricemia (HUA) has emerged as a global metabolic disorder that poses significant risks to human health. To investigate the effects and mechanisms of *Weizmannia coagulans* BC99 in alleviating hyperuricemia, we established a hyperuricemia mouse model. The results demonstrate that BC99 significantly downregulates the expression of uric acid (UA) reabsorption proteins in the kidneys and intestines, while upregulating the expression of UA excretion proteins. This modulation leads to a reduction in UA synthesis, mediated through the Nrf2/NLRP3 pathway. Additionally, BC99 intervention restored gut microbiota intestinal dysbiosis in HUA mice, increased the beneficial short-chain fatty acid (SCFA)-producing bacterial genera, and corrected disturbances in amino acid, purine, and pyrimidine metabolism. Collectively, our findings suggest that BC99 exhibits strong anti-hyperuricemic effects and holds promise as a dietary supplement for lowering uric acid levels.

Received 23rd February 2025,  
Accepted 7th April 2025

DOI: 10.1039/d5fo00951k

rsc.li/food-function

## 1. Introduction

Hyperuricemia (HUA) is a metabolic disorder resulting from either excessive production of uric acid (UA) or imbalanced excretion.<sup>1</sup> The prevalence of HUA has been steadily increasing worldwide, with higher rates observed in coastal regions. It is reported that approximately 20% of the individuals in the United States, 25% in Japan, and between 19% and 25% in Europe are affected by HUA.<sup>2</sup> Between 2018 and 2019, the prevalence of HUA among adults in China was observed to be 14%,<sup>3</sup> with a noticeable trend towards earlier onset.<sup>4</sup> Elevated UA levels can lead to conditions such as gout, chronic kidney disease, hypertension, and cardiovascular diseases.<sup>5–7</sup> UA is the final product of purine metabolism, primarily synthesized in the liver. Both excessive production and insufficient excretion of UA can disrupt serum UA homeostasis. The kidneys are the primary organs responsible for UA excretion,

accounting for approximately 70% of the total excretion, while the remaining 30% is eliminated through the intestines.<sup>8</sup> In the kidneys, uric acid is primarily reabsorbed by glucose transporter protein 9 (GLUT9) and uric acid transporter 1 (URAT1) and is subsequently excreted by ATP-binding cassette subfamily G member 2 (ABCG2) and organic anion transporters (OAT1 and OAT3).<sup>9</sup> Additionally, ABCG2 and GLUT9 also play roles in the excretion and reabsorption of uric acid through the gastrointestinal tract.<sup>10</sup> However, HUA often causes damage to the liver, kidneys, and gastrointestinal tract, likely due to inflammation and oxidative stress induced by elevated UA levels.<sup>11,12</sup> When the body experiences inflammation and oxidative stress, organ damage could occur, leading to altered expression of uric acid transporters. This alteration resulted in insufficient uric acid excretion, ultimately causing elevated levels of uric acid.<sup>13</sup> Currently, the main medications developed for treating hyperuricemia include allopurinol, febuxostat, and benzbromarone.<sup>14</sup> However, these drugs can cause adverse reactions, such as rash, severe allergic reactions, and renal toxicity, which may limit their clinical use.<sup>15</sup> Therefore, finding safe and effective alternatives for treating HUA is crucial.

Increasing evidence suggests that the gut microbiota plays a role in abnormal uric acid metabolism and systemic inflammation in HUA patients.<sup>16</sup> The gut microbiota not only participates in the metabolism of purines and uric acid but also produces short-chain fatty acids (SCFAs), which are essential for maintaining human health.<sup>17</sup> Dysbiosis of the gut microbiota can exacerbate intestinal inflammation and damage, leading to

<sup>a</sup>College of Food and Bioengineering, Henan University of Science and Technology, Luoyang, P.R. China. E-mail: shaobingu@haust.edu.cn, shaobingu@126.com; Tel: 86+0379-64283053; Fax: 86+0379-64283053

<sup>b</sup>Henan Engineering Research Center of Food Microbiology, Luoyang, P.R. China

<sup>c</sup>National Demonstration Center for Experimental Food Processing and Safety Education, Luoyang, P.R. China

<sup>d</sup>Germline Stem Cells and Microenvironment Lab, College of Animal Science and Technology, Nanjing Agricultural University, Nanjing, 210095, China

†Electronic supplementary information (ESI) available. See DOI: <https://doi.org/10.1039/d5fo00951k>

‡These authors contributed equally to this work.



inflammation in the kidneys and liver, ultimately causing organ dysfunction and worsening HUA.<sup>18</sup> Recent studies have shown that the gut microbiota is involved in purine and uric acid metabolism.<sup>19</sup> For example, the gut microbiota can secrete xanthine oxidase, which is involved in the oxidative metabolism of purines.<sup>20</sup> Thus, adjusting the gut microbiota may be a promising strategy for treating hyperuricemia. Numerous studies have demonstrated that probiotics can enhance the richness and diversity of the gut microbiota, thereby reducing the production of uric acid. For instance, research has shown that *Lactobacillus plantarum* LLY-606 can increase the abundance of beneficial bacteria such as *Akkermansia muciniphila*, *Lactobacillus plantarum*, and *Parabacteroides merdae*. By modulating the gut microbiota and its metabolites and inhibiting inflammation, *Lactobacillus plantarum* LLY-606 alleviates hyperuricemia. Additionally, *Lactobacillus paracasei* MJM60396 upregulates uric acid transporters, increases the expression of tight junction proteins such as ZO-1 and occludin, and significantly reduces serum uric acid levels to normal ranges. *Weizmannia coagulans* is a spore-forming, lactic acid-producing bacterium that is Generally Recognized As Safe (GRAS) by the U.S. Food and Drug Administration (FDA) and is considered an ideal probiotic for improving gut health. Although *W. coagulans* is not a natural resident of the gut, it can transiently inhabit the gastrointestinal tract and promote a beneficial balance of microbial community. This transience of *W. coagulans* in the gastrointestinal tract reduces the risk of developing opportunistic infections and pathogenicity-related gene transfer compared with other probiotics that adhere to and colonize the gastrointestinal epithelium. Its probiotic functions and stability during processing and storage have garnered significant attention from researchers and food manufacturers. Furthermore, *W. coagulans* can produce metabolic by-products such as diacetyl, SCFAs, digestive enzymes, and vitamins. It also stimulates intestinal peristalsis, reduces the production of harmful substances like amines, and improves the intestinal metabolic environment, thereby promoting healthy bowel movements and preventing the accumulation of toxins in the body.<sup>21</sup> Additionally, research has demonstrated that strains of *W. coagulans* play a crucial role in regulating the composition of the microbiota, enhancing immune function, and alleviating metabolic disorders.<sup>22–24</sup> These studies suggest that *W. coagulans* has potential to prevent and treat HUA.

This study established a HUA mouse model and employed epigenetic indicators and multi-omics analysis to reveal the mechanisms through which BC99 supplementation reduces HUA. The objectives are to (i) verify whether BC99 has a positive regulatory effect on HUA mice, (ii) assess whether BC99 supplementation can inhibit the activation of inflammatory signaling pathways and improve the expression of uric acid transporters in the kidney and intestine, and (iii) explore the potential relationship between the gut microbiota and differential metabolites and HUA. This is the first report on the effects of *Weizmannia coagulans* in reducing uric acid and its underlying mechanisms, offering a novel strategy for the treatment and prevention of hyperuricemia.

## 2. Materials and methods

### 2.1 Materials and reagents

The *W. coagulans* BC99 strain was obtained from Wecare Probiotics Co., Ltd (Suzhou, China). The following substances were purchased from Shanghai Aladdin Bio-Chem Technology Co., Ltd (Shanghai, China), hypoxanthine (HX, purity  $\geq 98\%$ ), potassium oxytetracycline (PO, purity  $\geq 98\%$ ), and carboxymethyl cellulose sodium (CMC-Na). The mouse interleukin-6 (IL-6), interleukin-1 beta (IL-1 $\beta$ ), tumor necrosis factor-alpha (TNF- $\alpha$ ), interleukin-18 (IL-18), and interleukin-10 (IL-10) ELISA kits were purchased from Nanjing Boyan Biotechnology Co., Ltd (Nanjing, China). The catalase (CAT), malondialdehyde (MDA), glutathione (GSH), superoxide dismutase (SOD), adenosine deaminase (ADA), xanthine oxidase (XOD), creatinine (Cr), and blood urea nitrogen (BUN) assay kits were purchased from Iseju (Lianyungang, Jiangsu) Biotechnology Co., Ltd (Jiangsu, China). The ALT and AST assay kits were purchased from Nanjing Jiancheng Bioengineering Institute (Nanjing, China). The UA assay kits were purchased from Shanghai Xinfan Biotechnology Co., Ltd. The BCA protein quantification assay kits were purchased from Beyotime Biotechnology Co., Ltd (Shanghai, China). The anti-ABCG2, anti-NLRP3, anti-Caspase-1, anti-Nrf2, anti-HO-1, anti-Keap1, and anti-IgG antibodies were all purchased from Wuhan Cloud-Clone Corp Co., Ltd (Wuhan, China). The anti- $\beta$ -actin antibody was purchased from Affinity Biosciences Co., Ltd (Jiangsu, China). Anti-GLUT9 antibodies were purchased from Proteintech Biotech Co., Ltd (Wuhan, China).

### 2.2 Establishment of the hyperuricemia mouse model and drug administration

Male ICR mice (6 weeks old) were purchased from SPF Biotechnology Co., Ltd (Beijing, China) and were housed under controlled conditions ( $22 \pm 2$  °C, 50% relative humidity, and a 12 h light/dark cycle). After a one-week adaptation period, the mice were randomly divided into 6 groups ( $n = 9$ ), as shown in Fig. 1A. All groups, except for the CON group, were fed a special diet containing 20% yeast extract (by system weight). All modeling drugs were prepared as solutions with 0.05% carboxymethyl cellulose sodium, and BC99 was resuspended in sterile saline. The CON group was gavaged with a 0.05% carboxymethyl cellulose sodium solution, while the other groups were gavaged with 280 mg kg<sup>-1</sup> potassium oxytetracycline and 100 mg kg<sup>-1</sup> hypoxanthine, based on body weight. Six hours later, the CON and HUA groups were gavaged with sterile saline, while the BL, BM and BH groups received 10<sup>6</sup>, 10<sup>7</sup> and 10<sup>8</sup> CFU per g body weight of bacteria, respectively. The AL group was administered allopurinol at 42 mg kg<sup>-1</sup>. All gavage doses were approximately 0.2 mL and were administered continuously for three weeks. During the treatment period, body weight and food intake were monitored every three days. At the end of the experiment, the mice were fasted for 12 hours before blood, liver, kidney, intestinal and cecal contents were collected and immediately stored at  $-80$  °C for subsequent analysis. All animal procedures were



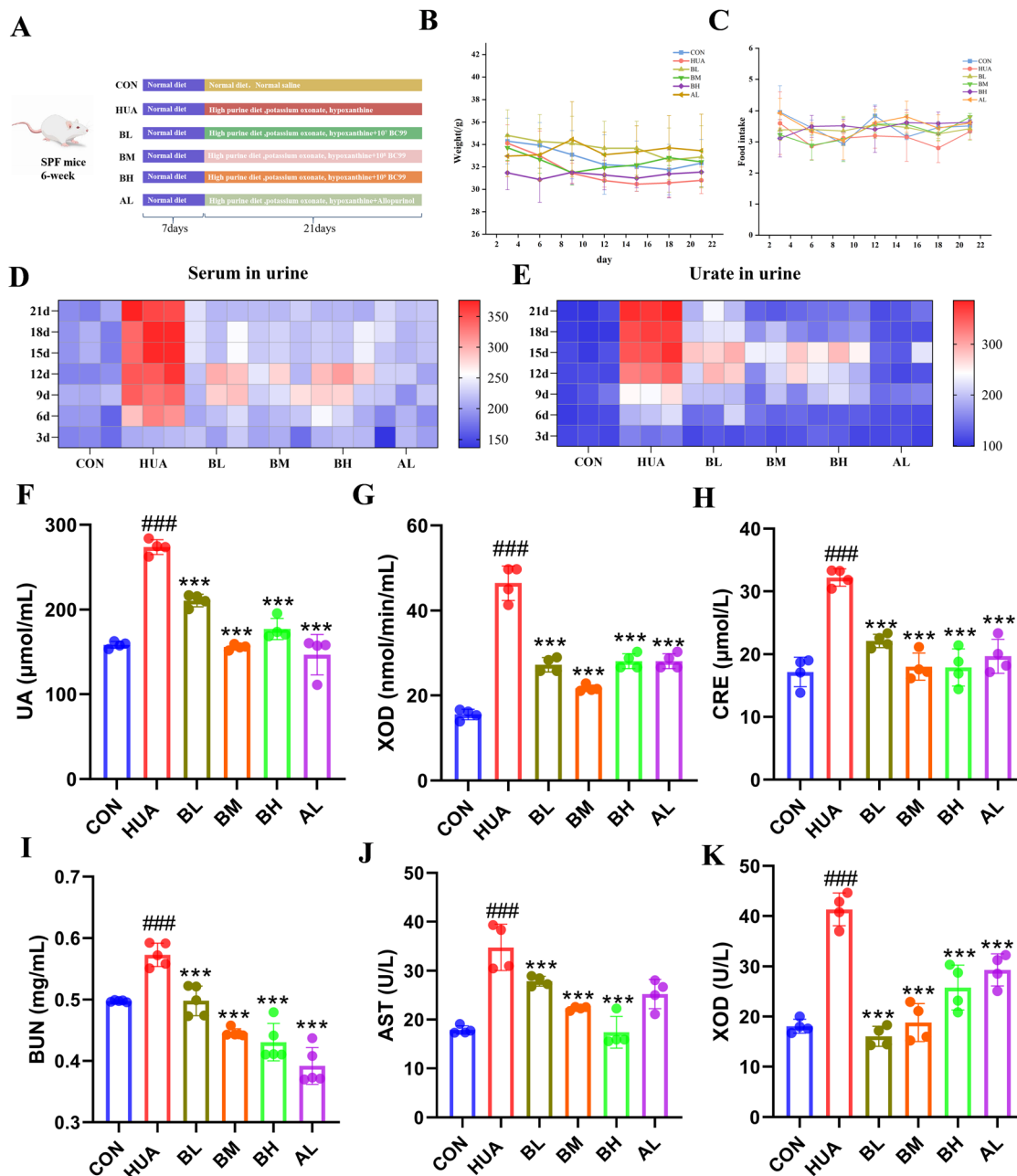


**Fig. 1** Effects of *Weizmannia coagulans* BC99 on serum indices in mice at different time points. (A) Schematic diagram of the study design. (B) Body weight. (C) Food intake. (D) Serum uric acid in urine. (E) Uric acid in urine. (F) Xanthine oxidase (XOD). (G) Creatinine (CRE). (H) Uric acid (UA). (I) Aspartate aminotransferase (AST). (J) Alanine aminotransferase (ALT). (K) Blood urea nitrogen (BUN). #, ## and ### represent  $p < 0.05$ ,  $0.01$  and  $0.001$  respectively, vs. the control group; \*, \*\* and \*\*\* represent  $p < 0.05$ ,  $0.01$  and  $0.001$  respectively, vs. the hyperuricemia model group.

approved by the Zhengzhou University Animal Ethics Committee (License No.: SCXK (Yu) 2022-0005).

### 2.3 Histopathological examination

Liver, kidney and intestinal samples from the mice were collected, rinsed with PBS, and then fixed in 4% paraformaldehyde. After embedding in paraffin and sectioning, the samples were fixed for 48 hours and stained with hematoxylin and eosin (H&E). Tissue pathological changes were observed under

an optical microscope (E100, Nikon Corporation, Japan) using bright-field illumination.

### 2.4 Immunohistochemical staining

Liver, kidney, and intestinal samples from the mice were harvested, rinsed with PBS, and fixed in 4% paraformaldehyde. After paraffin embedding and sectioning, the slides were subjected to baking, dewaxing, and rehydration. Antigen retrieval was performed in a citrate buffer (pH 6.0). The slides were



treated with 3% hydrogen peroxide to block endogenous peroxidase activity. Following PBS rinses, the primary antibody was applied and incubated overnight at 4 °C. After three PBS washes, the secondary antibody was added and incubated at room temperature for 20–30 min. The slides were then stained with DAB, counterstained with hematoxylin for 3 min, and washed. The slides were examined under a microscope, and the results were analyzed using ImageJ software.

### 2.5 Measurement of inflammatory factors

Mouse blood samples were centrifuged at 4 °C for 15 min at 4000 rpm to obtain plasma samples. The concentrations of IL-6, IL-1 $\beta$ , TNF- $\alpha$ , IL-18 and IL-10 in the plasma were measured using ELISA kits, following the instructions provided in the kit manuals.

### 2.6 Real-time PCR

Total RNA was isolated from the kidney and intestine samples using Trizol (Accurate Biology, Hunan, China) following the manufacturer's protocol. The extracted messenger RNA was then reverse transcribed into cDNA using a reverse transcription kit (Accurate Biology, Hunan, China). Quantitative real-time polymerase chain reaction (RT-PCR) was conducted to quantify gene expression, with cycle threshold values compared using the 2Ct method, actin served as the internal reference gene. Specific primers for each gene were custom-designed and synthesized by Sangon Biotechnology (Table 1).

### 2.7 16S rRNA sequencing analysis

At the end of the 21 day modeling period, the cecal contents were collected and placed into sterile centrifuge tubes, rapidly frozen in liquid nitrogen, and stored at -80 °C to prevent DNA degradation. DNA from various samples was isolated using the CTAB method, following the manufacturer's instructions. The V3–V4 hypervariable region of the bacterial 16S rRNA gene was amplified with primer pairs 341F (5'CCTACGGGNGGCWGCAG-3') and 805R (5'GACTACHVGGGTATCTAATCC-3'). The amplicon pools were prepared for sequencing, and the size and amount of the amplicon library were determined using the Agilent Bioanalyzer (Agilent, USA) and the Library Quantification Kit for Illumina (KapaBiosciences, Woburn,

MA, USA). The libraries were sequenced using the NovaSeq PE250 platform.

### 2.8 UPLC-Q-TRAP-MS/MS analysis

We utilized LC-MS for thorough targeted analysis (Biotree, Shanghai, China). The LC separation was performed using a UPLC System (H-Class, Waters), equipped with a Waters Atlantis Premier BEH 2-HILIC Column (1.7  $\mu$ m, 2.1 mm  $\times$  150 mm). The mobile phase A consisted of a mixture of H<sub>2</sub>O and acetonitrile (8 : 2), with 10 mmol L<sup>-1</sup> ammonium acetate, while the mobile phase B was a combination of H<sub>2</sub>O and acetonitrile (1 : 9) with 10 mmol L<sup>-1</sup> ammonium acetate. The pH of mobile phases A and B was adjusted to 9 using aqueous ammonia. The autosampler temperature was set at 8 °C, and the injection volume was 1  $\mu$ L. The raw data files from LC-MS were processed using SCIEX Analyst Work Station Software, and metabolite quantification was performed using BIOTREE Bio Bud.

### 2.9 Statistical analysis

The experiments were independently repeated three times. SPSS software was used for the analysis, and the results were presented as mean  $\pm$  standard deviation (SD). Data analysis was performed using GraphPad Prism software. One-way analysis of variance (ANOVA) was conducted to assess the significance of differences between means. Tukey's HSD or Bonferroni was used for correction.

## 3 Results

### 3.1 Effect of *W. coagulans* BC99 on physical signs and biochemical indices of HUA mice

To assess the influence of BC99 on HUA, a mouse model of hyperuricemia was established as shown in Fig. 1A. Fluctuations in body weight were monitored throughout the feeding period. Nine days after potassium oxytetracycline (PO) and hypoxanthine modeling, the weight of the HUA mice decreased significantly, but returned to normal after supplementation with probiotics (Fig. 1B and C). As expected, mice in the HUA group exhibited higher serum uric acid levels

**Table 1** Primers used for PCR and RT-PCR

Gene	Forward (5' $\rightarrow$ 3')	Reverse (5' $\rightarrow$ 3')
URAT1	GGTGCTGACCTGGAGCTATC	AGAGGCTGGCTGTGTTTCATC
GLUT9	ATGGCAGGTCACTACTGTCTG	CTCAATTCCTCCGGTGCTCA
OAT1	AACTTCACTGCCGCTATCCC	TTCCGGTTGTCCTTGCTTGT
OAT3	AACGGCAAGAAGGAGGAAGG	ATGGACACCCGGAACAAGTC
ABCG2	TAGGTCCGGTGTGCGAGTCA	TAGCACATCTCCCTCTGCGA
PPAR $\gamma$	CGCCAAGGTGCTCCAGAAGATG	AGGGTGAAGGCTCATATCTGTCTCC
NLRP3	AGCCTCAGGGCACAAA	TGGATGAAGCACATAGTAAACA
ASC	AGACCACCAGCCAAGACAAG	CTCCAGGTCCATCACCAGT
Caspase1	AACCACTCGTACAGTCTTGCC	CCAGATCTCCAGCAGCAACTTC
Nrf2	CTTTAGTCAGCGACAGAAGGAC	AGGCATCTGTTTTGGGAATGTG
HO-1	AGGTACACATCCAAGCCGAGA	CATCACCAGCTTAAAGCCTTCT
$\beta$ -Actin	GGTTGCCGCTCTTGTGTAGAC	TACCGACCATGACTCCTTGATGAC



compared to those receiving a normal diet (CON) (Fig. 1E). Nevertheless, there were no observable phenotypic alterations (e.g., body weight, kidney and liver weight to body weight ratios) among them (Fig. S1A–C†). To determine the potential differences in circulating uric acid in HUA mice with or without supplementation of *W. coagulans* BC99, uric acid levels in the serum and urine and urate in urine were monitored every three days. Interestingly, mice supplemented with coagulated *W. coagulans* BC99 showed lower serum uric acid levels from day 18 onwards compared to the HUA mice (Fig. 1D and E), with a trend similar to that of the allopurinol treatment group. Meanwhile, the therapeutic effects of *W. coagulans* BC99 on liver and kidney damage in mice with hyperuricemia were examined. The findings demonstrated a significant increase in the serum levels of CRE, BUN, ALT, and AST in the hyperuricemic mice, while the addition of BC99 notably reduced the levels of these serum markers in hyperuricemic mice ( $p < 0.001$ ) (Fig. 1F–K), among them, the BM group exhibited the most significant effect. This phenomenon may be attributed to BC99 reaching its maximum efficacy within a certain dosage range, resulting in no further significant increase in the effect at higher doses.

### 3.2 Effects of *W. coagulans* BC99 on uric acid metabolism enzyme activity

The liver is a crucial organ for decomposition, metabolism, and detoxification, and is also the primary organ for synthesizing purine nucleotides in the body.<sup>25</sup> As shown in Fig. 2A, the livers of mice in the MOD group exhibited abnormal coloration and lost their luster, while the livers of mice in the other groups appeared bright red. H&E staining also showed that a large number of fat vacuoles appeared in the cytoplasm of HUA mice, indicating that liver cells were damaged and the ability to transport and metabolize fat decreased (Fig. 2B). In contrast, the liver cells treated with BC99 showed considerable improvement in structural disarray, reflecting a better organization of liver cords. Xanthine oxidase (XOD) is a rate-limiting enzyme in purine and nucleotide metabolism pathways and is the most important biological protease regulating uric acid production. As shown in Fig. 2C and D, the activities of ADA and XOD in the livers of HUA mice were significantly increased compared to the CON group. AL, as an XOD inhibitor, notably reduced the activity of uric acid synthesis-related enzymes in the livers of HUA mice ( $p < 0.001$ ). Compared to the HUA group, the activities of ADA and XOD in the livers of mice treated with three different doses of BC99 were significantly reduced ( $p < 0.001$ ). Additionally, UA-mediated oxidative stress damage led to the depletion of antioxidants, causing disordered fatty acid oxidation in liver cell mitochondria, substantial deposition of free fatty acids in the liver, lipid peroxidation of liver cell membranes, and an increase in MDA production.<sup>26</sup> As shown in Fig. 2E–H, compared with the CON group, the SOD, CAT and GSH contents of the HUA group decreased significantly, while the MDA content increased significantly. The SOD levels of the BC99 low, medium and high dose groups increased by 33.73%, 31.94% and 40.3% compared with the

HUA group. The GSH level increased by 15%, 25% and 10% compared with the HUA group, and the CAT level increased by 10.32%, 15% and 16.61% compared with the HUA group. These increases in antioxidant enzyme activities indirectly reflected BC99's ability to scavenge hepatic oxygen free radicals, while changes in MDA levels indicated BC99's effectiveness in inhibiting lipid peroxidation. This suggests that BC99 demonstrated a strong hepatoprotective effect by alleviating oxidative stress damage and reducing the activity of liver synthesis enzymes in HUA mice.

### 3.3 *W. coagulans* BC99 restored the altered expression level of UA transporters and suppressed inflammation in the kidneys of HUA mice

HUA is often accompanied by kidney damage.<sup>27</sup> Thus, we first used serum biochemical parameters and histopathological examination to investigate the effects of BC99 on renal function in HUA mice. The kidneys of the HUA mice are shown in Fig. 3A and appeared pale and noticeably enlarged with white spots; in both BC99 groups, however, the kidneys recovered to being reddish and smooth. It is noteworthy that the kidneys in the AL group were enlarged, which is consistent with previous studies showing that allopurinol treatment can cause kidney damage.<sup>28</sup> H&E staining revealed that the HUA group exhibited significant degeneration and necrosis of renal tubular epithelial cells, along with marked inflammatory cell infiltration in the interstitium. BC99 intervention at various doses demonstrated dose-dependent ameliorative effects on these pathological changes (Fig. 3B). These findings showed that *W. coagulans* BC99 supplementation had a beneficial effect and was safe for lowering blood urate levels. To assess the influence of the kidney on the reabsorption and excretion of uric acid, we employed RT-PCR analysis and IHC to analyze the expression of uric acid reabsorption and excretion transporters in the kidney. As shown in Fig. 3C, D and G, there was a remarkable increase in the expression of UA reabsorption proteins GLUT9 and URAT1, while UA excretion proteins ABCG2, OAT1 and OAT3 showed a significant decrease in the model group ( $p < 0.01$ ). These findings were in line with previous research.<sup>29</sup>

Previous studies have confirmed a connection between HUA and renal inflammation, leading to severe kidney damage.<sup>30</sup> Furthermore, the inflammatory response was decreased by blocking the activation of the NLRP3 inflammasome and activating the Nrf2 signaling pathway.<sup>31,32</sup> To explore the possible mechanisms, the gene expressions of Nrf2, HO-1, NLRP3, caspase-1, and ASC were examined. As shown in Fig. 3H, the mRNA expression of NLRP3, caspase1, ASC, Nrf2, and HO-1 in hyperuricemia model mice was considerably higher than that in the CON group. However, supplementation with BC99 treatment significantly reduces the mRNA expression of NLRP3, caspase1, ASC, Nrf2, HO-1 in the kidneys ( $p < 0.05$ ). Similarly, IHC results indicated that the HUA group upregulated the protein expressions of NLRP3 and caspase-1. The intervention with BC99 reversed this phenomenon (Fig. 3E and F). This suggested that the Nrf2/HO-1/



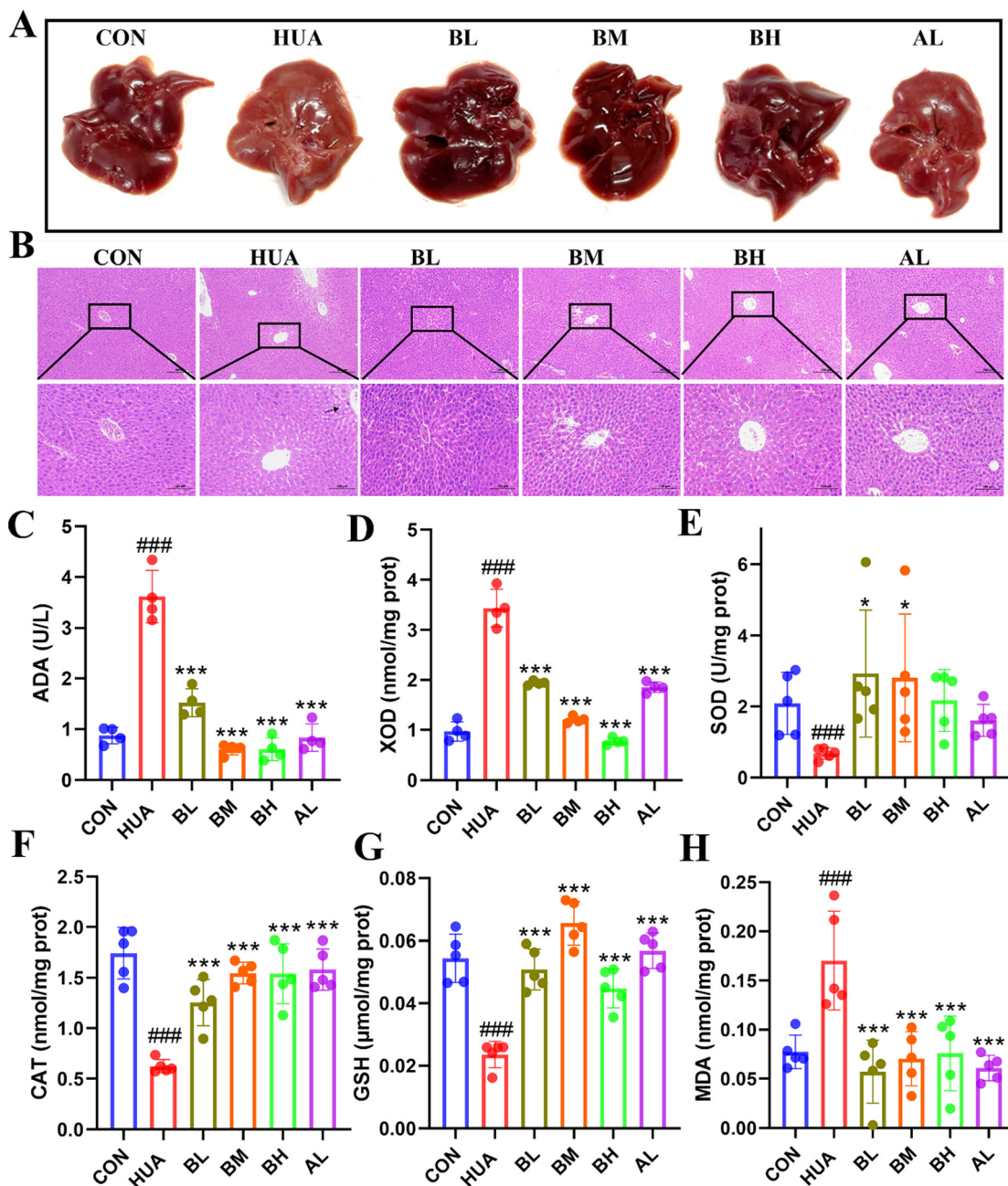


**Fig. 2** *Weizmannia coagulans* BC99 alleviated liver damage in hyperuricemic mice. (A) Appearance of the liver. (B) Hematoxylin and eosin staining of the liver. (C and D) Liver enzyme activities. (E) Superoxide dismutase (SOD) concentration. (F) Catalase (CAT) concentration. (G) Glutathione (GSH) concentration. (H) Malondialdehyde (MDA) concentration. #, ## and ### represent  $p < 0.05$ ,  $0.01$  and  $0.001$  respectively, vs. the control group; \*, \*\* and \*\*\* represent  $p < 0.05$ ,  $0.01$  and  $0.001$  respectively, vs. the hyperuricemia model group.

NLRP3 pathway might be involved in the uric acid-lowering effects mediated by BC99. In addition, the expression of inflammatory factors such as IL-1 $\beta$ , IL-6, IL-18 and TNF- $\alpha$  continued to be up-regulated in the kidneys of HUA mice (Fig. 3I), and the level of the anti-inflammatory factor IL-10 was significantly down-regulated ( $p < 0.001$ ). BC99 administration inhibited the elevated levels of IL-1 $\beta$ , IL-6, IL-18 and TNF- $\alpha$ , in the hyperuricemia mouse kidney ( $p < 0.001$ ). These results indicated that BC99 could alleviate renal inflammation in HUA

mice by activating Nrf2 expression and inhibiting the activation of the NLRP3 inflammasome in the kidneys. This, in turn, reduced inflammation and the expression of downstream inflammatory factors such as IL-1 $\beta$ , IL-6, IL-18, and TNF- $\alpha$ . Additionally, BC99 exerted a nephroprotective effect by upregulating the expression of renal transporters OAT1, OAT3, and ABCG2, while downregulating GLUT9 and URAT1 levels, thereby decreasing uric acid production and renal tubular damage.



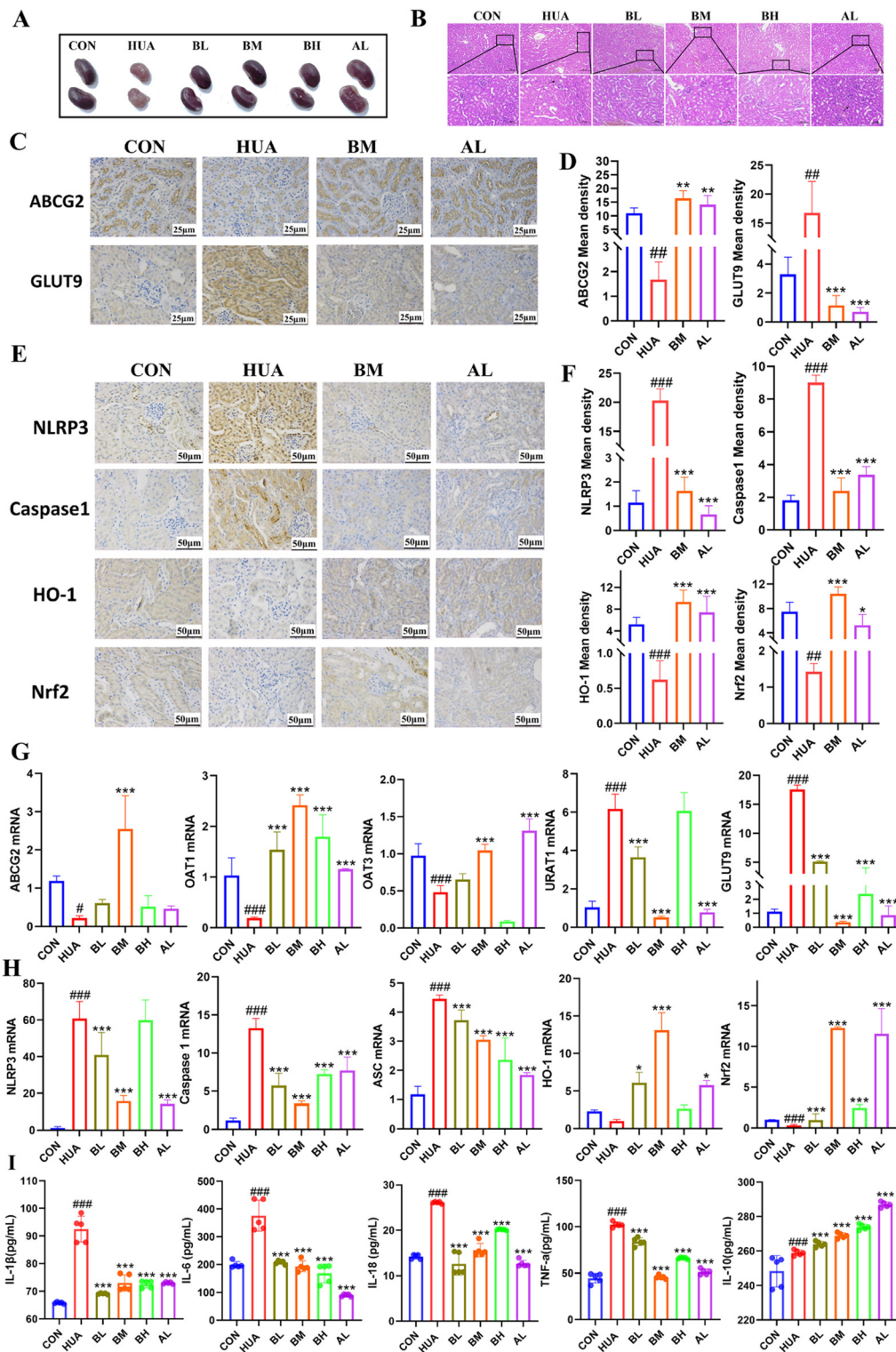


**Fig. 3** *Weizmannia coagulans* BC99 reversed the aberrant expression of uric acid (UA) transporter proteins and suppressed inflammation in the kidney of hyperuricemic mice. (A) Renal appearance. (B) Hematoxylin and eosin staining of kidneys. (C) Immunohistochemistry (IHC) images of ABCG2, GLUT9. (D) The mean density of ABCG2 and GLUT9. (E) IHC images of NLRP3, Caspase1, Nrf2 and HO-1. (F) The mean density of NLRP3, Caspase1, Nrf2 and HO-1. (G) The gene expression of ABCG2, GLUT9, OAT1, OAT3 and URAT1. (H) The gene expression of NLRP3, Caspase1, ASC, Nrf2 and HO-1. (I) Serum levels of interleukin-1 beta (IL-1 $\beta$ ), interleukin-6 (IL-6), interleukin-18 (IL-18), tumor necrosis factor-alpha (TNF- $\alpha$ ), and interleukin-10 (IL-10). #, ## and ### represent  $p < 0.05$ , 0.01 and 0.001 respectively, vs. the control group; \*, \*\* and \*\*\* represent  $p < 0.05$ , 0.01 and 0.001 respectively, vs. the hyperuricemic model group.



### 3.4 *W. coagulans* BC99 reduces intestinal damage and dysfunction in hyperuricemic mice

The bowel plays an important role in excreting uric acid.<sup>10</sup> Nonetheless, various studies have demonstrated that high levels of uric acid could cause damage to the intestines.<sup>33</sup> Therefore, H&E staining was conducted to evaluate the extent of intestinal damage. Compared to the CON group, the HUA group exhibited villous atrophy, looseness, shedding of epithelial cells in the intestinal lumen, and separation of the sub-mucosa. After intervention with BC99, improvements were observed to varying degrees in all groups, with the BM group showing the most significant effect. This indicated that BC99 could alleviate intestinal damage in mice with hyperuricemia (Fig. 4A). Mucosal damage could increase intestinal permeability and affect the intestinal mechanical barrier. This study found that the levels of lipopolysaccharides (LPS) were significantly elevated in the HUA group mice. Abnormal LPS not only damaged the intestinal barrier but also reduced the expression of tight junction proteins and induced pro-inflammatory responses in the gut (Fig. 4E).<sup>34</sup> To assess the intestinal barrier, tight junction proteins ZO-1 and Occludin were analyzed using IHC. Compared to the CON group, the HUA group showed a significant decrease in ZO-1 and Occludin levels ( $p < 0.001$ ). However, BC99 intervention effectively inhibited this decrease ( $p < 0.01$ ). The consistency of these results indicated that BC99 could mitigate intestinal damage in mice, protect intestinal epithelial cells, and partially maintain the integrity of the intestinal mucosa. To investigate the effect of BC99 on intestinal UA excretion, we measured the gene expression levels of ABCG2 and GLUT9. As shown in Fig. 4D, the expression of ABCG2 in the intestines of HUA mice was significantly reduced, while GLUT9 expression was significantly increased ( $p < 0.05$ ). BC99 treatment at all three doses reversed these trends. In addition, the results of this study found that supplementation with *W. coagulans* BC99 could upregulate ABCG2 transcription by activating PPAR $\gamma$ , which is consistent with the study by Xu *et al.*<sup>35</sup> (Fig. 4D) ( $p < 0.05$ ). Immunohistochemistry revealed a significant increase in ABCG2 and a significant decrease in GLUT9 in the BC99 treatment groups, with the BM group showing the most pronounced effects. Additionally, the BM group demonstrated a more extensive promotion of UA excretion in the intestines compared to the AL group (Fig. 4D) ( $p < 0.05$ ). Interestingly, we observed that compared to the CON group, the colons of HUA mice were shorter (Fig. S2A $\dagger$ ) and displayed alterations in H&E staining images (Fig. S2B $\dagger$ ). Multiple lines of evidence suggested that inflammation in the mice was exacerbated, leading to edema and shortening of the colon.<sup>36,37</sup> Similar to the findings in the kidneys, levels of NLRP3, caspase-1, and ASC in the intestines were significantly upregulated ( $p < 0.001$ ), whereas moderate doses of BC99 significantly inhibited these levels. In addition, BC99 intervention activated the expression of Nrf2 and HO-1 (Fig. 4H). These results suggest that BC99 can promote intestinal uric acid excretion by activating the expression of Nrf2 and inhibiting NLRP3 activation.

### 3.5 *W. coagulans* BC99 ameliorated gut microbiota dysbiosis in hyperuricemic mice

The variances in the gut microbiota among cohorts were assessed through the sequencing of the bacterial 16S rRNA gene. The gut microbiome plays a crucial role in preserving intestinal equilibrium and managing gastrointestinal function.<sup>38</sup> We analyzed the gut microbiota of HUA mice and explored the impact of BC99 intervention on the gut microbiota of patients with HUA mice. Fig. 5A represents the species accumulation curve. The curve tends to plateau, indicating the reasonableness of the sequencing data. The sequencing results indicate that the overwhelming majority of bacterial species information in this experimental sample is suitable for further analysis of bacterial community diversity and species composition. The Venn diagram demonstrates a clear distinction in the makeup of the six OTU groupings (Fig. 5B). The number of OTUs in the HUA group decreased compared with that in the CON group, whereas it recovered after BC99 group. Alpha diversity analysis showed no significant differences between the groups (Fig. 5C and D). Principal coordinate analysis (PCoA) was used to examine community composition and detect potential changes in the gut microbiota structure. Furthermore, the beta diversity score revealed changes in the architecture of mouse flora among groups. These findings revealed that the organization of the intestinal flora was radically different in the mice from three groups (Fig. 5E and F). Based on the unweighted species abundance data, the samples were clustered using the unweighted pair group method with arithmetic mean (UPGMA). The inter-sample distances were computed to evaluate how similar the species compositions were between the samples. The results revealed that BC99 intervention induced the microbiota structure of hyperuricemic mice to become similar to that of the animals in the normal group (Fig. 5F). Fig. 5G–M depicts the alterations in intestinal flora at the phylum level in mice from various groups. The probiotic intervention group exhibited a reduction in the presence of Verrucomicrobia and Bacteroidetes, while an increase was observed in the abundance of Firmicutes, Proteobacteria, and Actinobacteriota. The composition of the intestinal flora at the genus level showed that *Hungatella*, *Escherichia-Shigella* and *Lachnoclostridium* had a dramatically higher percentage in the HUA group (pathogenic bacteria that lead to elevated uric acid levels) than that of the CON group, while the percentage of (beneficial bacteria) *Lachnospiraceae\_NK4A136\_group*, *Pseudoflavonifractor*, *Muribaculaceae\_unclassified*, *Lactobacillus*, *Enterorhabdus*, *Alistipes*, *Burkholderia-Caballeronia-Paraburkholderia*, *Alloprevotella*, and *Clostridium* significantly decreased. And probiotic supplementation reversed these changes again (Fig. 5L–S).

LefSe analysis was performed to explore the key microbiota of the changes among the groups. As presented in Fig. 6A and B, the pathogenic bacteria *Hungatella* and *Bacteroides* were significantly enriched in the HUA group, while potentially beneficial short-chain fatty acid-producing microbes, such as



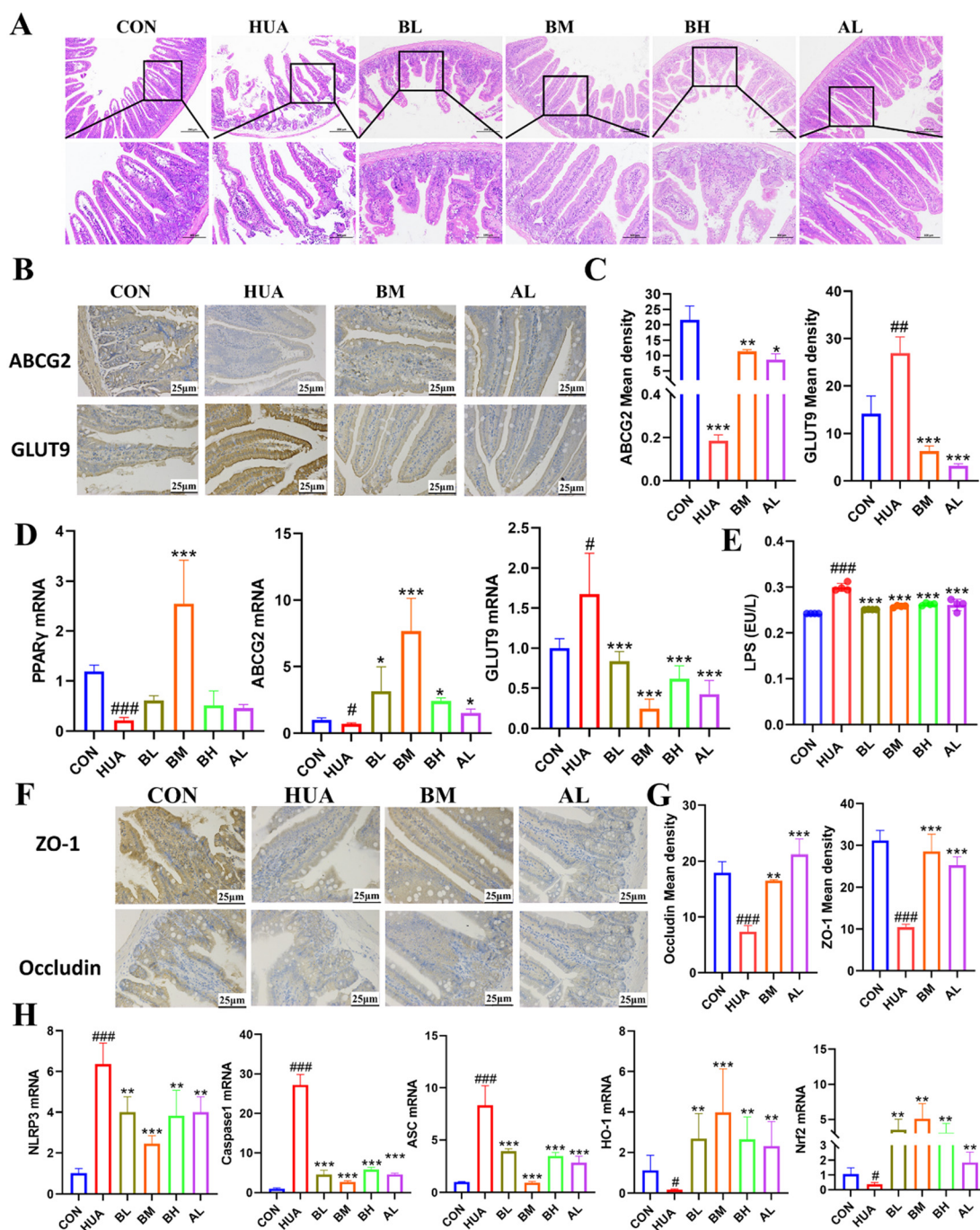


**Fig. 4** *Weizmannia coagulans* BC99 relieved the intestinal damage and dysfunction of hyperuricemic mice. (A) Hematoxylin and eosin staining of the intestine. (B) Immunohistochemistry (IHC) images of ABCG2 and GLUT9. (C) The mean density of ABCG2 and GLUT9. (D) The gene expression of PPAP $\gamma$ , ABCG2 and GLUT9, (E) LPS. (F) IHC images of the intestinal mechanical barrier (occludin and ZO-1). (G) The mean density of ZO-1 and occluding. (H) Expression levels of NLRP3, Caspase1, ASC, Nrf2 and HO-1. #, ## and ### represent  $p < 0.05$ , 0.01 and 0.001 respectively, vs. the control group; \*, \*\* and \*\*\* represent  $p < 0.05$ , 0.01 and 0.001 respectively, vs. the hyperuricemia model group.

*Alloprevotella*, *Enterorhabdus*, *Lactobacillus*, *Lachnospiraceae\_NK4A136\_group*, and *Blautia*, were enriched in the BC99 group. Additionally, by analyzing the correlations between the gut microbiota and inflammatory factors and oxidative stress, the study identified key bacterial strains in BC99 that alleviate inflammation and oxidative stress in HUA mice. At the

genus level, *Bacteroides*, *Parabacteroides*, *Lachnospiraceae*, *Escherichia-Shigella*, and *Acetatifactor* were positively correlated with pro-inflammatory cytokines and oxidative stress markers. Conversely, *Prevotellaceae\_UCG-001*, *Muribaculaceae\_unclassified*, *Bacillus*, *Anaerotruncus*, and *Enterorhabdus* played roles in alleviating inflammation and oxidative stress. These strains



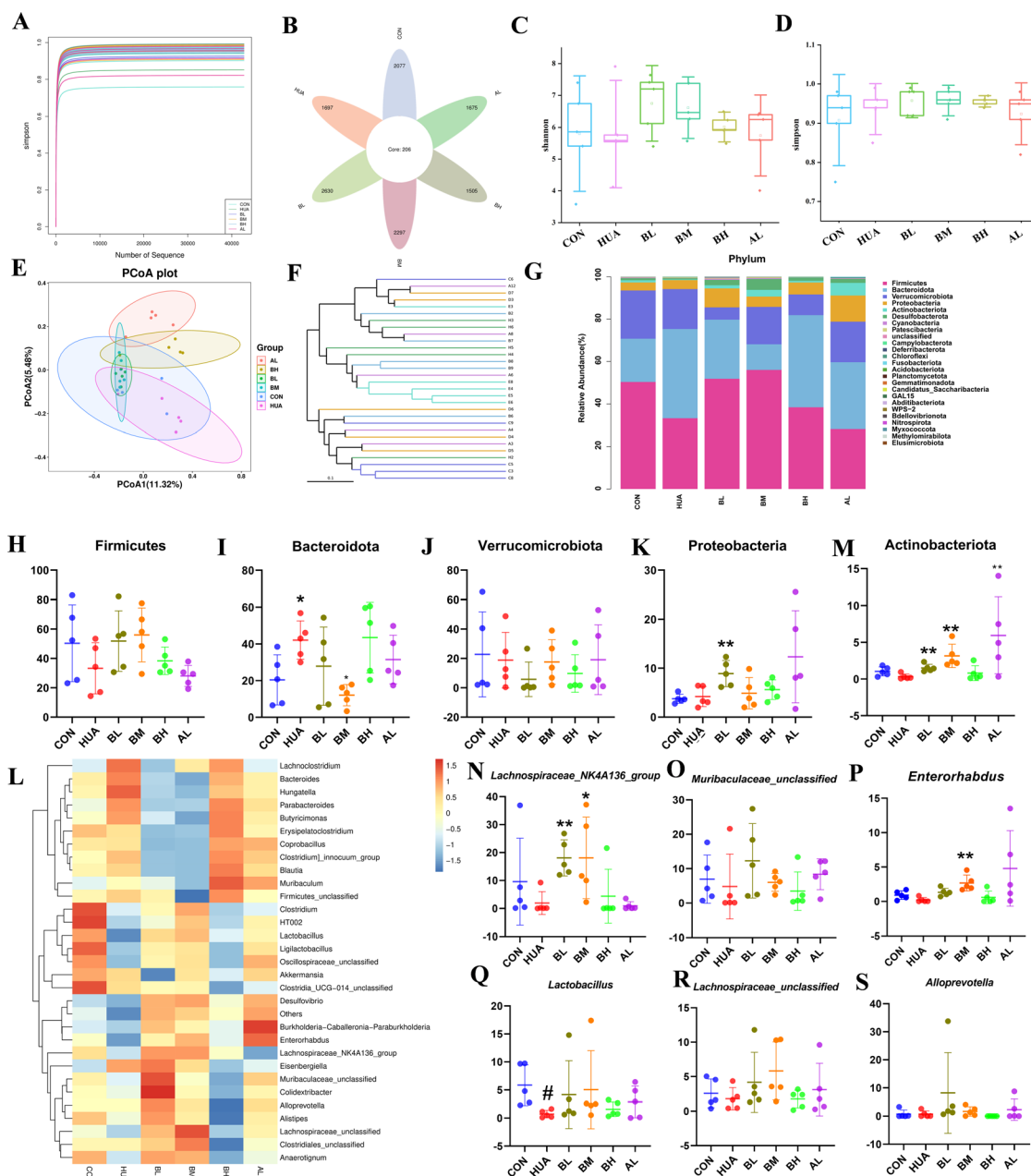


**Fig. 5** The effect of *Weizmannia coagulans* BC99 on the regulation of the intestinal microbial structure and composition in hyperuricemic mice. (A) Sparse curves reflecting  $\alpha$ -diversity at different sequencing depths. (B) Venn diagrams of OTU illustrating the overlap among groups. (C and D) A box chart of the alpha diversity illustrating the diversity of each group. (E) The plot of principal co-ordinate analysis (PCoA). (F) The plot of UPGMA clustering analysis. (G–M) Phylum level. (L–S) Genus level. \*  $p < 0.05$ , \*\*  $p < 0.01$ .

showed significant negative correlations with pro-inflammatory cytokines and oxidative stress markers and positive correlations with anti-inflammatory factors and antioxidant enzymes (Fig. 6C).

### 3.6 Effect of BC99 intervention on the relationship between SCFA levels and microbiota in hyperuricemic mice

Short-chain fatty acids (SCFAs) are by-products generated through the fermentation process of beneficial gut microbiota bacteria, primarily comprising acetate, propionate, and buty-

rate. These fatty acids play a crucial role in regulating both gut and systemic immunity and are closely associated with diet, microbiota, and antibiotic use.<sup>39</sup> Compared to the CON group, the levels of acetic acid, propionic acid, isovaleric acid, butyric acid, valeric acid, and isobutyric acid were significantly reduced in the HUA group ( $p < 0.001$ ). In contrast, after BC99 treatment, SCFA levels notably increased, with significant elevations in acetic acid, propionic acid, and isobutyric acid, especially in the BM group (Fig. 6D). These results suggest that BC99 may alleviate HUA by increasing SCFA levels.



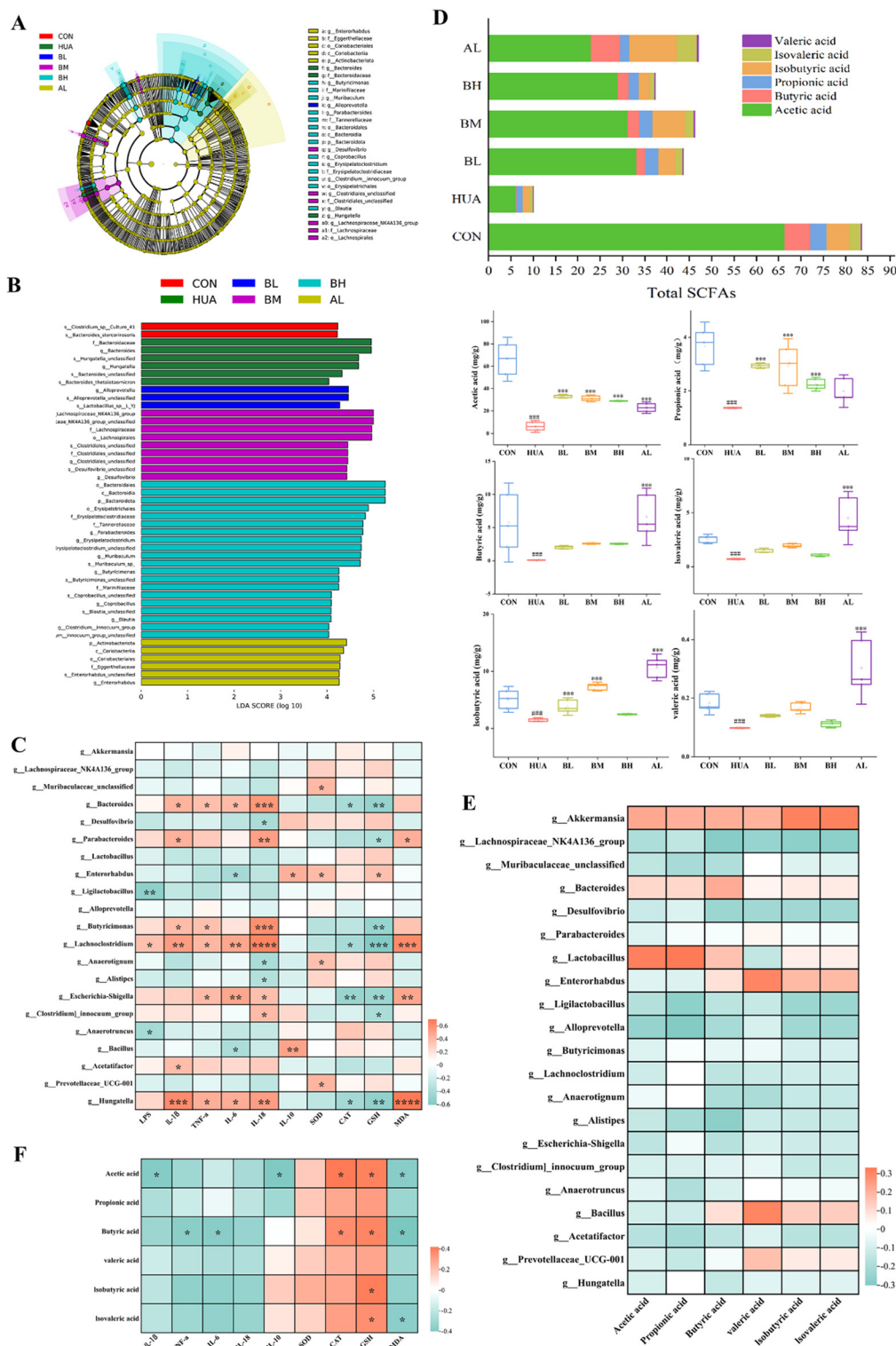


**Fig. 6** (A) Cladogram. (B) Distribution histogram based on LDA (LDA score > 4.0). (C) Heatmap of the correlation between gut flora and inflammatory factors and oxidative stress. (D) SCFA content. (E) Heatmap of the correlation between gut flora and SCFAs. (F) Correlation heat map of SCFAs and inflammatory factors and oxidative stress. \*  $p < 0.05$ , \*\*  $p < 0.01$ , \*\*\*  $p < 0.001$ .

Additionally, Pearson correlation analysis revealed a positive correlation between SCFAs and the gut microbiota genera *Enterorhabdus*, *Akkermansia*, *Bacillus*, *Prevotellaceae UCG-001*,

and *Lactobacillus* (Fig. 6E). The analysis of the relationship between SCFAs and inflammatory markers and oxidative stress indicators revealed a positive association between acetic acid,



propionic acid, butyric acid, valeric acid, isobutyric acid, and isovaleric acid with antioxidant enzymes, while showing a negative correlation with inflammatory factors (Fig. 6F). These findings indicate that SCFAs can modulate the expression of inflammatory cytokines and antioxidant enzymes and that BC99's anti-uric acid effects are closely related to its role in reshaping the gut microbiota and regulating its microbial metabolites.

### 3.7 Extensive targeted metabolomics analysis of differential metabolites and pathways in HUA mice

Through the use of comprehensive targeted serum metabolomics, combined with multivariate statistical analysis and bioinformatics analysis, the study explored the effects of BC99 on the metabolic characteristics of HUA mice. It identified potential biomarkers and corresponding metabolic pathways associated with the anti-hyperuricemia effects and elucidated the potential mechanisms of action of BC99 in combating high uric acid levels. Principal Component Analysis (PCA) and Orthogonal Partial Least Squares Discriminant Analysis (OPLS-DA) were both used for multivariate statistical analysis on 340 metabolites in this investigation. PCA, an unsupervised model, was used to uncover the internal structure of the data, thereby providing a clearer interpretation of the data variables.<sup>40</sup> The PCA score plots revealed distinct separations between the CON and HUA groups, as well as between the HUA and BC99 groups (Fig. 7A and B), indicating that BC99 intervention significantly affected the metabolites in HUA mice. Orthogonal Projections to Latent Structures Discriminant Analysis (OPLS-DA) was then utilized for statistical analysis in order to get more trustworthy data on the inter-group variations in metabolites and their significance to the experimental groups. Consistent with the PCA results, clear separations were observed between the CON and HUA groups and between the HUA and BC99 groups (Fig. 7C and D). The  $R^2Y$  and  $Q^2$  values are crucial parameters for the OPLS-DA model; values closer to 1 indicate greater reliability of the model. In this study, the  $R^2Y$  value of the OPLS-DA model was 0.98, indicating that the model was effectively established with good explanatory and predictive power (Fig. S3A–B†). Based on the above analyses and considering both univariate and multivariate statistical results, metabolites with  $P < 0.05$  and  $VIP > 1$  were selected as differential metabolites. These results are presented in the form of a volcano plot. As shown in Fig. 7E, compared to the CON group, the HUA group exhibited significant upregulation of 6 differential metabolites and significant downregulation of 10 differential metabolites. Compared to the HUA group, BC99 intervention resulted in significant upregulation of 16 differential metabolites and significant downregulation of 27 differential metabolites (Fig. 7F). Furthermore, these differential metabolites were categorized into 15 groups (Fig. 7G), with the major categories being amino acids, peptides, and analogues (28.824%), organic acids and derivatives (13.529%), carbohydrates and carbohydrate conjugates (12.059%), nucleosides, nucleotides, and analogues (8.824%), benzenoids (7.059%), and biogenic amines (6.765%). This dis-

tribution indicates the crucial role played by these substances in the anti-hyperuricemic effects of BC99. Subsequently, the quantitative values of the differential metabolites were used to calculate corresponding ratios, which were then log-transformed with base 2. The top 10 significantly upregulated and downregulated metabolites were selected. As shown in Fig. 7H and I, the  $x$ -axis displays the log-transformed fold changes, and the color intensity of the points represents the VIP values. Compared to the CON group, the HUA group exhibited significant downregulation of differential metabolites such as 2-methylglutaric acid, *N6,N6,N6*-trimethyl-*L*-lysine, cortisone, acetaminophen, trigonelline, and 1,1-dimethyl-prolinium. Conversely, metabolites like pantothenic acid, orotic acid, and 3,4-dihydroxymandelic acid were significantly upregulated. Following BC99 intervention, there was a notable upregulation of differential metabolites such as 3-(3-hydroxyphenyl) propanoic acid, trigonelline, and 1,1-dimethyl-prolinium. These findings further support the conclusion that BC99 improves metabolic disturbances in HUA mice. Subsequently, Pearson correlation analysis was performed to assess the associations between these differential metabolites and biochemical indicators, inflammatory factors, and oxidative stress markers. Interestingly, pantothenic acid, orotic acid, 3,4-dihydroxymandelic acid, *N*-carbamoyl-*L*-aspartate, and octopamine showed positive correlations with inflammatory factors and liver and kidney damage indicators, and negative correlations with anti-inflammatory factors and antioxidant enzymes. In contrast, 3-(3-hydroxyphenyl)propanoic acid, trigonelline, 1,1-dimethyl-prolinium, 2-methylglutaric acid, and mesaconic acid were negatively correlated with inflammatory factors and liver and kidney damage indicators, and positively correlated with anti-inflammatory factors and antioxidant enzymes. Research has indicated that 3-(3-hydroxyphenyl)propanoic acid (PPA) has potential biological activity in stimulating the differentiation and proliferation of osteoblasts in cell culture.<sup>41</sup> In addition, the correlation analysis between differential metabolites and the gut microbiota revealed that 3-(3-hydroxyphenyl) propanoic acid was positively correlated with beneficial bacteria (such as *Lachnospiraceae\_NK4A136\_group*, *Muribaculaceae\_unclassified*, *Enterorhabdus*, *Anaerotignum*, *Alistipes*, *Anaerotruncus*, and *Prevotellaceae\_UCG-001*) and negatively correlated with the pathogenic bacterium *Hungatella*. These results suggest that changes in these potential biomarkers may alter associated metabolic pathways, thereby improving metabolic disturbances and reducing uric acid levels in HUA mice. Then, in order to determine which major pathways were most strongly linked to metabolite differences, a thorough investigation of the pathways connected to the differential metabolites was carried out, utilizing topological and enrichment analyses.<sup>42</sup> The name of the KEGG metabolic route is shown by the ordinate, and the abscissa shows the RichFactor associated with each pathway. The number of differential metabolites enriched in the route is indicated by the size of the dots. The color corresponds to the magnitude of the  $p$  value. A smaller  $p$  value results in a deeper red color, indicating a higher level of enrichment. As shown in Fig. 7L, the main enriched metabolic



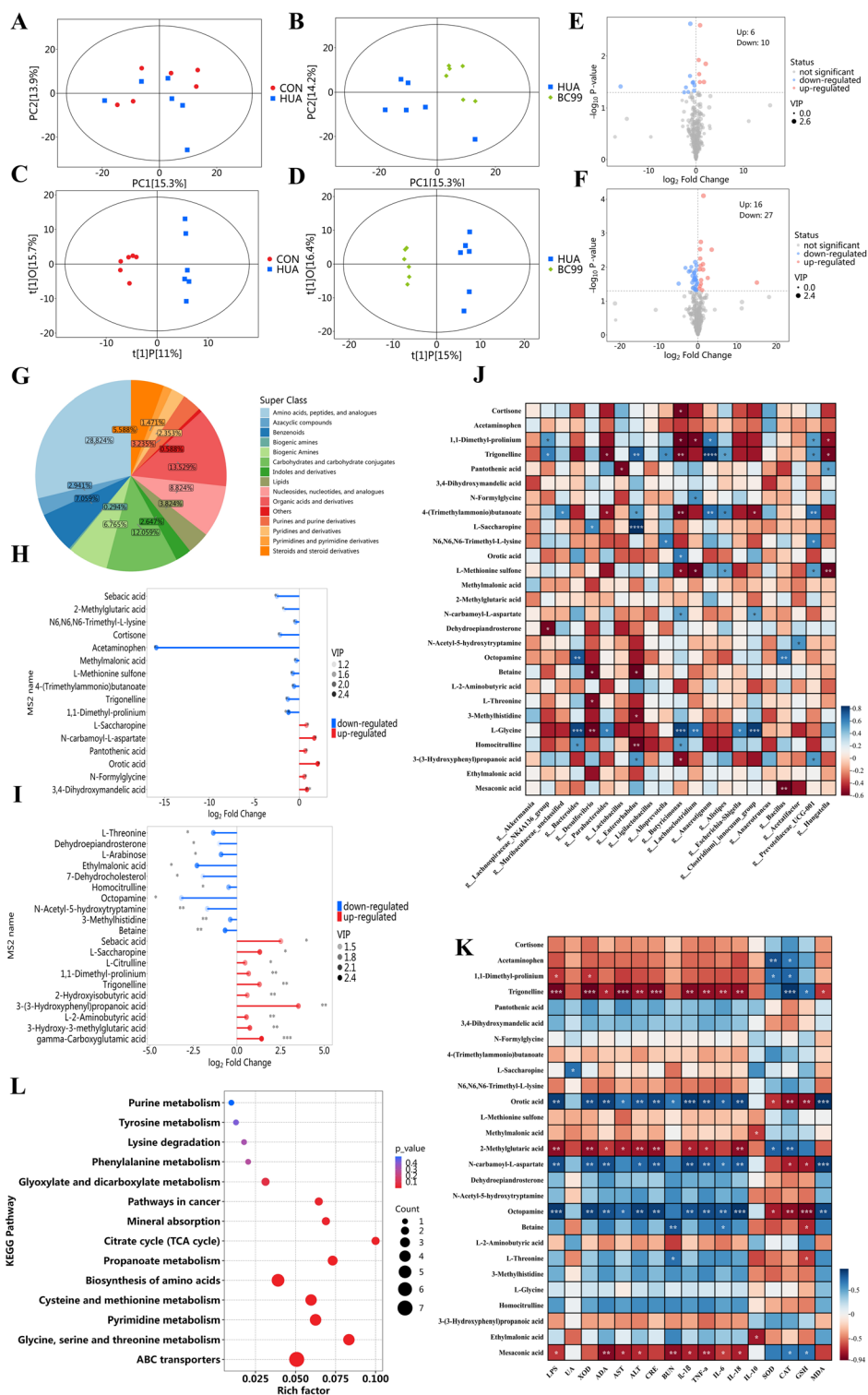


**Fig. 7** (A) PCA score diagram of the CON group and HUA group in ESI+ mode and ESI- mode. (B) PCA score diagram of the HUA group in ESI+ mode and ESI- mode. (C) OPLS-DA score diagram of the CON group and HUA group in ESI+ mode and ESI- mode. (D) OPLS-DA score diagram of the HUA group and BC99 group in ESI+ mode and ESI- mode. (E) Volcano plot (CON/MOD). (F) Volcano plot (HUA/BC99). (G) Pie chart of metabolite classification. (H) Matchstick plot analysis of differential metabolites (CON/HUA). (I) Matchstick plot analysis of differential metabolites (HUA/BC99). (J) Correlation analysis between different bacterial genera and different metabolites. (K) Correlation analysis between differential metabolites and biochemical indicators. (L) KEGG enrichment map of differential metabolites in different groups.



pathways were amino acid metabolism, especially glycine, serine, and threonine metabolism.

### 3.8 The construction and analysis of the metabolic mechanism network for potential biomarkers and related metabolic pathways were carried out

There was a certain connection between pyrimidine metabolism and high uric acid levels. Pyrimidines and purines are products of RNA and DNA, playing important roles in cellular energy metabolism and signal transduction.<sup>43</sup> In terms of pyrimidine metabolism, deoxycytidine and orotic acid were identified as metabolites with disrupted levels. UMP is an intermediate of deoxycytidine and orotic acid, with deoxycytidine being a major nucleoside in DNA. Orotic acid serves as an intermediate in the pyrimidine nucleotide synthesis pathway. The levels of orotic acid can significantly increase in conditions such as certain genetic urea cycle enzyme deficiencies, ammonia overload due to high-protein diets, and abnormalities in arginine metabolism. These conditions might indirectly affect the production and excretion of uric acid by influencing metabolic pathways in the body. As shown in Fig. 8, compared to the CON group, the HUA group showed increased levels of orotic acid. After treatment with BC99, the disrupted pyrimidine metabolism returned to normal levels. A recent study also indicated that metabolites related to pyrimidine metabolism were significantly dysregulated in patients with hyperuricemia and gout.<sup>44</sup> This finding is consistent with the results of this study.

Amino acids are essential for the growth and development of organisms, with certain amino acids acting as critical regu-

latory factors in key metabolic pathways.<sup>45</sup> Changes in amino acid metabolism are closely associated with inflammation.<sup>46</sup> In terms of amino acids, the metabolism of tyrosine is particularly important. Sodium urate (MSU) stimulates an increase in tyrosine levels, activates neutrophils and the tyrosine kinase Tec, and induces the release of IL-1 $\beta$ , IL-8, and tyrosine, thereby triggering an inflammatory response.<sup>47</sup> Elevated tyrosine levels in the body can also impact the activity of enzymes like citrate synthase, malate dehydrogenase, and succinate dehydrogenase in the tricarboxylic acid cycle, resulting in disturbance of mitochondrial energy metabolism and oxidative stress.<sup>48</sup> In this study, elevated levels of tyrosine and decreased levels of phenylalanine were observed in the HUA group, indicating that excess uric acid disrupts the biosynthesis of phenylalanine, tyrosine, and tryptophan by accelerating the conversion of phenylalanine to tyrosine. However, after BC99 intervention, tyrosine levels were reduced and phenylalanine levels were increased. This suggests that BC99 may alleviate inflammation and lower uric acid levels by modulating the metabolic pathways of phenylalanine and tyrosine. 3-(3-Hydroxyphenyl) propanoic acid is a hydroxylated phenylalanine metabolite with various biological activities. For instance, 3HPPA exhibits strong vasodilatory potential in rats and has anti-inflammatory and antioxidant effects in RAW264.7 cells.<sup>49</sup> In this study, the level of 3-(3-hydroxyphenyl) propanoic acid was significantly reduced in the HUA group, and this trend was reversed with BC99 intervention. Additionally, research has shown that dietary L-lysine can prevent adenine-induced arterial calcification in uremic rats.<sup>50</sup> A higher intake of lysine helps reduce

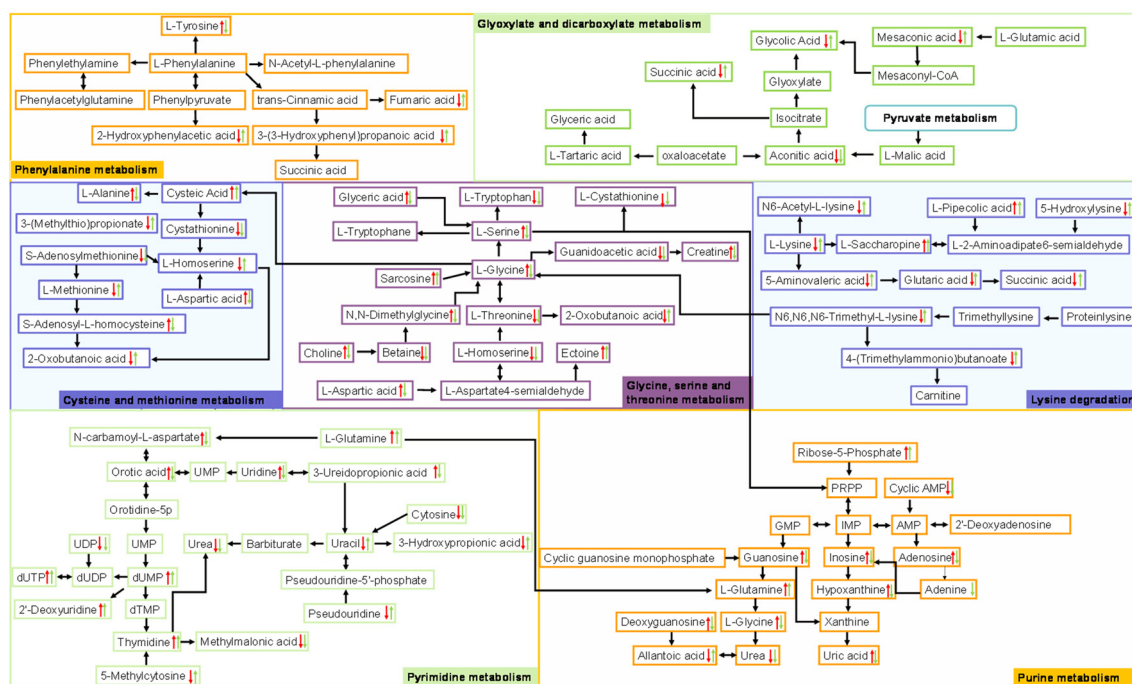


Fig. 8 The intervention of *Weizmannia coagulans* on the metabolism of HUA mice. The red arrows represent the trend of metabolite changes in HUA rats, and the green arrows represent the trend of metabolite shift after BC99 intervention.



the risk of hyperuricemia, while a decrease in L-lysine levels may increase the risk of cardiovascular diseases.<sup>51,52</sup> The results of this study found that L-lysine levels were significantly reduced in the HUA group of mice, and BC99 intervention reversed this effect. Glyoxylic acid and dicarboxylic acid metabolism is a biochemical pathway involving the synthesis and degradation of a series of organic acids, which is particularly significant in microorganisms. Additionally, kynurenic acid (KYNA), a metabolite derived from the kynurenine pathway of tryptophan catabolism, exerts immunoregulatory effects on macrophages.<sup>53</sup> This suggests that kynurenic acid may regulate immune responses by affecting specific stages in dicarboxylic acid metabolism, such as  $\beta$ -oxidation or  $\omega$ -oxidation. Additionally, research has shown that kynurenic acid exerts anti-inflammatory effects by reducing the expression of LPS-induced inflammatory factors, such as IL-1 $\beta$ , IL-6, and IL-10.<sup>54</sup> This indicates that kynurenic acid may influence inflammation by affecting the activity of certain enzymes or metabolic fluxes in the dicarboxylic acid metabolism pathway. Additionally, succinic acid has been shown to exert anti-inflammatory, antioxidant, and neuroprotective effects. Although current research has not definitively established a direct link between glyoxylic acid and dicarboxylic acid metabolism pathways and the development of hyperuricemia (HUA), this pathway is significantly associated with lipid metabolism, amino acid metabolism, and various other processes.<sup>55</sup> Studies have indicated that serine is involved in the metabolism of glyoxylic acid and dicarboxylic acids. Serine is an important intermediate in these metabolic pathways. Elevated levels of serine may saturate certain metabolic enzymes, leading to the accumulation of intermediate products in the metabolic pathways, which in turn affects cellular energy metabolism and other metabolic processes. Additionally, serine metabolism can produce pyruvate, an intermediate in the tricarboxylic acid (TCA) cycle. Pyruvate can further be converted into precursors of uric acid, such as phosphoribosyl pyrophosphate (PRPP). Increased serine metabolism may lead to the accumulation of PRPP, thereby increasing uric acid production. Furthermore, cysteine can be synthesized from methionine or serine *via* the transsulfuration pathway. During its breakdown, cysteine can release a thiol group and an amino group, producing pyruvate. In this study, increased levels of L-serine were observed in the serum of the HUA group mice, while BC99 intervention significantly reduced these levels. This suggests that BC99 may inhibit inflammation and oxidative stress and reduce uric acid production by regulating metabolites related to amino acid metabolism.

## 4. Discussion

Mounting evidence suggests that HUA is caused by either overproduction or insufficient excretion of uric acid.<sup>56</sup> URAT1 is the primary transport protein responsible for reabsorbing urate from the blood, and it is expressed on the apical surface of renal tubular cells.<sup>57</sup> GLUT9 is also considered to play a crucial role in uric acid reabsorption, primarily located on

both the basolateral and apical membranes.<sup>58</sup> OAT1, OAT3, and ABCG2 primarily regulate the excretion of uric acid from the blood into the proximal tubular lumen and are located on the apical brush border and basolateral membranes, respectively.<sup>59</sup> Defects in these uric acid transport proteins lead to the occurrence of hyperuricemia,<sup>60,61</sup> further supporting their role as effective targets for the prevention and treatment of HUA. Additionally, ABCG2 and GLUT9 are crucial for intestinal uric acid excretion.<sup>62</sup> Therefore, uric acid transport proteins in these two organs are considered the most promising and effective targets for treating hyperuricemia. Furthermore, the liver is the primary organ responsible for uric acid synthesis.<sup>63</sup> Elevated uric acid levels increase liver lipid accumulation, induce oxidative stress, and trigger inflammatory responses. However, no studies have reported the simultaneous uric acid-lowering effects of *W. coagulans* on the liver, kidneys, and intestines. In this study, *W. coagulans* BC99 was found to significantly reduce the levels of hepatic uric acid synthase, decrease the expression of URAT1 and GLUT9 in the kidneys of hyperuricemia model mice, and increase the expression of PPAR $\gamma$ , ABCG2, OAT1, and OAT3 (Fig. 9). Additionally, the gut microbiota can increase the excretion of uric acid by secreting intestinal transport proteins, promote the regeneration and repair of intestinal epithelial tissue cells, and alter the number and distribution of uric acid transport proteins in intestinal epithelial cells. Recent research indicated that activating PPAR $\gamma$  could upregulate the transcription of ABCG2.<sup>35</sup> This study found that BC99 intervention can activate the expression of intestinal PPAR $\gamma$ , thereby upregulating the transcription of ABCG2 and increasing the excretion of uric acid. Interestingly, this study found that BC99 was more effective than allopurinol in significantly regulating the expression of uric acid transport proteins in the kidneys and intestines of hyperuricemia model mice. These results suggest that BC99 might have superior anti-hyperuricemic effects compared to allopurinol, as it could simultaneously reduce uric acid production and promote uric acid excretion in the kidneys and intestines. However, further research is needed to elucidate how BC99 improves the expression of uric acid transport proteins in the kidneys and intestines.

HUA is often accompanied by inflammation and oxidative stress. Research findings suggest that uric acid and monosodium urate (MSU) crystals may exacerbate organ damage and malfunction by inducing inflammation and triggering inflammatory signaling pathways.<sup>64</sup> IL-1 $\beta$ , IL-18, IL-6, and TNF- $\alpha$ , as pro-inflammatory cytokines, are commonly observed cytokines in the early stages of uric acid-induced inflammation.<sup>65</sup> Inhibiting these inflammatory cytokines has been considered an effective approach for treating uric acid-related conditions. In this study, the serum levels of pro-inflammatory cytokines were significantly elevated in HUA model mice, while the anti-inflammatory cytokine IL-10 was significantly reduced. Caspase-1 and IL-1 $\beta$  are important markers of NLRP3 activation.<sup>66</sup> The activation of the NLRP3 inflammasome also results from ASC oligomerization.<sup>67</sup> Under MSU stimulation, the NLRP3 protein recruits the adaptor protein ASC, which



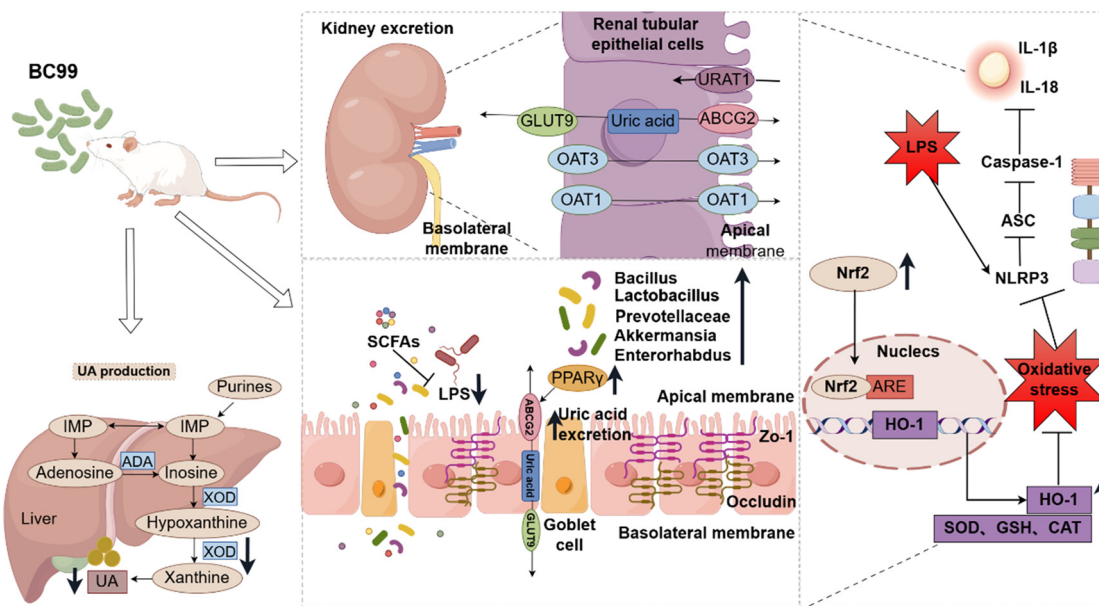


**Fig. 9** Potential mechanism of action of *Weizmannia coagulans* BC99 in alleviating HUA. BC99 intervention increased the abundance of SCFA-producing bacteria, thereby producing more SCFAs. SCFAs activated the Nrf2 pathway, inhibited the activation of NLRP3, and reduced the secretion of proinflammatory cytokines. This reduced the expression of uric acid reabsorption proteins, increased the expression of UA excretion proteins, and reduced the synthesis of UA. Furthermore, BC99 restored amino acid and purine-pyrimidine metabolism homeostasis in hyperuricemic mice.

further recruits pro-caspase-1. Once pro-caspase-1 on the inflammasome precursor is cleaved into caspase-1, it activates a biologically active mature NLRP3 inflammasome, thereby mediating the extensive production of cytokines. Our study indicated that the inflammatory NLRP3 pathway was activated in the kidneys and intestines of HUA mice. In contrast, the administration of BC99 significantly reduced the levels of proinflammatory cytokines in the serum of HUA mice and inhibited NLRP3 activation in the kidneys and intestines. These findings are consistent with previous research.<sup>68–70</sup> Nrf2 is a key transcription factor that maintains redox balance by preserving redox homeostasis.<sup>71</sup> Nrf2 translocates into the cell nucleus to induce the expression of the HO-1 protective protein, thereby alleviating inflammation mediated by the NLRP3 inflammasome.<sup>72</sup> In this study, BC99 significantly increased the nuclear translocation of Nrf2, thereby upregulating HO-1 protein levels and reducing oxidative stress. Additionally, H&E staining analysis showed that BC99 effectively alleviated liver, kidney, and intestinal damage in hyperuricemic mice. These results indicated that BC99 could mitigate inflammatory damage in the kidneys and intestines of HUA mice and reduce oxidative stress. Furthermore, the study found that the expression of uric acid transport proteins was influenced by the inflammatory NLRP3 signaling pathway. Zhang *et al.* demonstrated that fucoidan could effectively inhibit the induction of uric acid transport proteins URAT1 and GLUT9 by suppressing the activation of NF- $\kappa$ B, JNK, and PI3K/Akt signaling pathways in HK-2 cells.<sup>73</sup> Han *et al.* also found that ellagic acid could restore the expression of uric acid transport proteins through the MAPK/NF- $\kappa$ B signaling

pathway.<sup>69</sup> This study demonstrated that BC99 could significantly inhibit NLRP3 in the kidneys and intestines of hyperuricemic mice, activate Nrf2 expression, and thereby restore the expression of uric acid transport proteins. However, these findings have not yet been directly validated through functional experiments (*e.g.*, Nrf2 knockout or NLRP3 inhibitors) to establish causal relationships. Elucidating this mechanistic detail will be a key focus of future research.

Increasing data indicate that the gut microbiota and its metabolites are critical mediators of the liver–kidney–intestine axis, playing a fundamental role in human health.<sup>74</sup> The gut barrier prevents hazardous chemicals from entering the systemic circulation.<sup>75</sup> The homeostasis of the gut microbiota is closely related to intestinal permeability.<sup>76</sup> In this work, BC99 repaired the structural morphology of the intestines and boosted the expression levels of intestinal tight junction proteins in HUA mice. It also alleviated intestinal inflammation, damage, and dysfunction, thereby promoting uric acid excretion. Furthermore, we discovered that the BC99 treatment increased the relative abundance of *Firmicutes* while decreasing the number of *Bacteroidetes*, which is consistent with the findings of Cao *et al.*<sup>77</sup> Existing studies have shown that gut microbiota-derived SCFAs can alleviate hyperuricemia by inhibiting inflammation and promoting intestinal uric acid excretion.<sup>78</sup> *Akkermansia* is a bacterium that produces SCFAs and can improve metabolic health by increasing SCFA levels. *Lactobacillus*, *Prevotellaceae*, and *Bacillus* can modulate the gut microbiota and SCFA levels, thereby reducing inflammatory responses.<sup>79</sup> *Enterorhabdus* is a beneficial gut bacterium with various positive effects. It can promote the metabolism of poly-



phenols and carbohydrates in the intestine, thereby contributing to the maintenance of intestinal health.<sup>80</sup> Additionally, in the treatment of colorectal cancer (CRC), *Enterorhabdus* has been found to increase the levels of butyrate and isovalerate. These metabolites have positive effects on intestinal health and cancer prevention.<sup>81</sup> This study found that bacteria producing SCFAs were positively correlated with SCFAs and significantly reduced in the hyperuricemia mouse model. BC99 treatment effectively increased the abundance of these beneficial bacteria. Additionally, SCFAs had a negative correlation with pro-inflammatory cytokines and a favorable correlation with anti-inflammatory and antioxidant enzymes. In contrast, the abundance of the harmful gut bacterium *Hungatella* significantly increased in the HUA group and was positively correlated with inflammatory factors and oxidative stress markers, while negatively correlated with SCFAs. Therefore, the increase in *Hungatella* may contribute to renal dysfunction through various mechanisms. Overall, BC99 may alleviate hyperuricemia and reduce inflammation and oxidative stress by remodeling the gut microbiota. However, the beneficial effects of BC99 on hyperuricemia through the gut microbiota require further validation through gut microbiota transplantation experiments.

Extensive studies have revealed a direct relationship between HUA and metabolic diseases.<sup>82</sup> Metabolomics is increasingly used to diagnose diseases and understand their underlying mechanisms.<sup>83</sup> Broad-targeted metabolomics technology, as an emerging technique combining both untargeted and targeted metabolomics approaches, offers advantages over traditional metabolomics techniques in terms of broader coverage and higher sensitivity.<sup>84</sup> Here, we conducted a broad-targeted metabolomics study of serum to assess metabolic differences between HUA mice that received and did not receive BC99 treatment. Metabolomics analysis revealed that, compared to the CON group, multiple pathways were significantly dysregulated in the HUA group. Metabolites such as guanosine, inosine, and adenosine in the purine metabolism pathway were significantly elevated in hyperuricemic mice, but these levels were reduced following BC99 treatment. In addition to purine and pyrimidine metabolism, metabolites involved in amino acid metabolism and glyoxylate and dicarboxylate metabolism were also significantly dysregulated. Interestingly, these metabolic pathways are primarily interconnected through amino acids, with glycine, serine, and threonine metabolism appearing to be key nodes. Glycine, serine, and threonine are important precursors for protein synthesis, nucleic acids, and lipids, with glycine and serine also serving as precursors for uric acid. In this study, glycine and serine were significantly elevated in the HUA group, leading to excessive uric acid production and ultimately resulting in hyperuricemia. BC99 was able to significantly reverse these metabolic pathways. This effective action may be attributed to glycine and serine participating in various biosynthetic pathways and stress responses, channeling energy into other metabolic pathways (such as glyoxylate and dicarboxylate metabolism, and cysteine and methionine metabolism). This, in turn, produces

beneficial metabolites that alleviate inflammatory responses and reduce HUA. Therefore, we speculate that hyperuricemia may stimulate amino acid metabolism dysregulation, exacerbating the condition. BC99 effectively reversed the amino acid metabolism disturbances, suggesting that its protective effect against HUA may be partly attributed to the improvement of amino acid metabolism. Furthermore, the beneficial effects of BC99 on HUA through the regulation of amino acid metabolism require further validation.

This study confirmed that BC99 treatment can reduce purine synthesis, improve the expression of transport proteins in the kidneys and intestines by inhibiting inflammatory signaling pathways and enhancing oxidative stress. Additionally, BC99 can correct gut microbiota dysbiosis and restore purine and amino acid metabolism imbalances in hyperuricemic mouse models. This research provides important insights and directions for studying the mechanisms of BC99 in lowering uric acid and offers a theoretical basis for its application in preventing and treating HUA. Future studies will further validate the relationship between metabolite changes and the uric acid-lowering mechanisms through cellular experiments and other biotechnological approaches.

## Author contributions

Ying Wu: formal analysis, data curation, writing – review & editing, supervision, and funding acquisition. Yinyin Gao: conceptualization, methodology, writing – original draft, formal analysis, and investigation. Cheng Li: methodology, software, and writing – review & editing. Shirui Zhai: validation and resources. Yao Dong: validation and resources. Shanshan Tie: data curation, supervision, and writing – review & editing. Lina Zhao: software and writing – review. Shaobin Gu: data curation, writing – review & editing, supervision, and funding acquisition.

## Ethics statements

All mouse experiments were approved by the Zhengzhou University Animal Ethics Committee (License No.: SCXK (Yu) 2022-0005).

## Data availability

Data will be made available on request.

## Conflicts of interest

The authors declare that they have no known competing financial interests or personal relationships that could have appeared to influence the work reported in this paper.



## Acknowledgements

This study was financially supported the Major Science and Technology Special Projects in Henan Province (Grant No. 231100310200); the Key R&D Projects in Henan Province (Grant No. 241111314200 and 221111111400); and the National Natural Science Foundation of China (Grant No. 32302069).

## References

- 1 L. A. B. Joosten, T. O. Crişan, P. Bjornstad and R. J. Johnson, Asymptomatic hyperuricaemia: a silent activator of the innate immune system, *Nature reviews, Rheumatology*, 2020, **16**, 75–86.
- 2 M. Chen-Xu, C. Yokose, S. K. Rai, M. H. Pillinger and H. K. Choi, Contemporary Prevalence of Gout and Hyperuricemia in the United States and Decadal Trends: The National Health and Nutrition Examination Survey, 2007–2016, *Arthritis Rheumatol.*, 2019, **71**, 991–999.
- 3 K. Li, K. Li, Q. Yao, X. Shui, J. Zheng, Y. He and W. Lei, The potential relationship of coronary artery disease and hyperuricemia: A cardiometabolic risk factor, *Heliyon*, 2023, **9**, e16097.
- 4 A. Mehmood, L. Zhao, C. Wang, M. Nadeem, A. Raza, N. Ali and A. A. Shah, Management of hyperuricemia through dietary polyphenols as a natural medicament: A comprehensive review, *Crit. Rev. Food Sci. Nutr.*, 2019, **59**, 1433–1455.
- 5 N. Dalbeth, A. L. Gosling, A. Gaffo and A. Abhishek, Gout, *Lancet*, 2021, **397**, 1843–1855.
- 6 H. He, P. Guo, J. He, J. Zhang, Y. Niu, S. Chen, F. Guo, F. Liu, R. Zhang, Q. Li, S. Ma, B. Zhang, L. Pan, G. Shan and M. Zhang, Prevalence of hyperuricemia and the population attributable fraction of modifiable risk factors: Evidence from a general population cohort in China, *Front. Public Health*, 2022, **10**, 936717.
- 7 M. Dehlin, L. Jacobsson and E. Roddy, Global epidemiology of gout: prevalence, incidence, treatment patterns and risk factors, *Nature reviews, Rheumatology*, 2020, **16**, 380–390.
- 8 A. Mehmood, L. Zhao, M. Ishaq, W. Xin, L. Zhao, C. Wang, I. Hossen, H. Zhang, Y. Lian and M. Xu, Anti-hyperuricemic potential of stevia (*Stevia rebaudiana* Bertoni) residue extract in hyperuricemic mice, *Food Funct.*, 2020, **11**, 6387–6406.
- 9 H. Yanai, H. Adachi, M. Hakoshima, S. Iida and H. Katsuyama, A Possible Therapeutic Application of the Selective Inhibitor of Urate Transporter 1, Dotinurad, for Metabolic Syndrome, Chronic Kidney Disease, and Cardiovascular Disease, *Cells*, 2024, **13**, 450.
- 10 X. Xu, C. Li, P. Zhou and T. Jiang, Uric acid transporters hiding in the intestine, *Pharm. Microbiol.*, 2016, **54**, 3151–3155.
- 11 Y. H. Chang, Y. F. Chiang, H. Y. Chen, Y. J. Huang, K. L. Wang, Y. H. Hong, M. Ali, T. M. Shieh and S. M. Hsia, Anti-Inflammatory and Anti-Hyperuricemic Effects of Chrysin on a High Fructose Corn Syrup-Induced Hyperuricemia Rat Model via the Amelioration of Urate Transporters and Inhibition of NLRP3 Inflammasome Signaling Pathway, *Antioxidants*, 2021, **10**, 564.
- 12 J. Chen, L. Xu, L. Jiang, Y. Wu, L. Wei, X. Wu, S. Xiao, Y. Liu, C. Gao, J. Cai and Z. Su, Sonneratia apetala seed oil attenuates potassium oxonate/hypoxanthine-induced hyperuricemia and renal injury in mice, *Food Funct.*, 2021, **12**, 9416–9431.
- 13 Y. H. Lu, Y. P. Chang, T. Li, F. Han, C. J. Li, X. Y. Li, M. Xue, Y. Cheng, Z. Y. Meng, Z. Han, B. Sun and L. M. Chen, Empagliflozin Attenuates Hyperuricemia by Upregulation of ABCG2 via AMPK/AKT/CREB Signaling Pathway in Type 2 Diabetic Mice, *Int. J. Biol. Sci.*, 2020, **16**, 529–542.
- 14 S. Li, H. Yang, Y. Guo, F. Wei, X. Yang, D. Li, M. Li, W. Xu, W. Li, L. Sun, Y. Gao and Y. Wang, Comparative efficacy and safety of urate-lowering therapy for the treatment of hyperuricemia: a systematic review and network meta-analysis, *Sci. Rep.*, 2016, **6**, 33082.
- 15 J. S. Lee, J. Won, O. C. Kwon, S. S. Lee, J. S. Oh, Y. G. Kim, C. K. Lee, B. Yoo and S. Hong, Hepatic Safety of Febuxostat Compared with Allopurinol in Gout Patients with Fatty Liver Disease, *J. Rheumatol.*, 2019, **46**, 527–531.
- 16 J. Wang, Y. Chen, H. Zhong, F. Chen, J. Regenstein, X. Hu, L. Cai and F. Feng, The gut microbiota as a target to control hyperuricemia pathogenesis: Potential mechanisms and therapeutic strategies, *Crit. Rev. Food Sci. Nutr.*, 2022, **62**, 3979–3989.
- 17 N. Yamada, C. Iwamoto, H. Kano, N. Yamaoka, T. Fukuuchi, K. Kaneko and Y. Asami, Evaluation of purine utilization by *Lactobacillus gasseri* strains with potential to decrease the absorption of food-derived purines in the human intestine, *Nucleosides, Nucleotides Nucleic Acids*, 2016, **35**, 670–676.
- 18 P. Liu, J. Yang, Y. Chen, Y. Zhu, Y. Tang, X. Xu and H. He, Alterations of gut microbiota and metabolome in early chronic kidney disease patients complicated with hyperuricemia, *Heliyon*, 2023, **9**, e20328.
- 19 Z. Guo, J. Zhang, Z. Wang, K. Y. Ang, S. Huang, Q. Hou, X. Su, J. Qiao, Y. Zheng, L. Wang, E. Koh, H. Danliang, J. Xu, Y. K. Lee and H. Zhang, Intestinal Microbiota Distinguish Gout Patients from Healthy Humans, *Sci. Rep.*, 2016, **6**, 20602.
- 20 J. K. Crane, T. M. Naeher, J. E. Broome and E. C. Boedeker, Role of host xanthine oxidase in infection due to enteropathogenic and Shiga-toxicogenic *Escherichia coli*, *Infect. Immun.*, 2013, **81**, 1129–1139.
- 21 E. P. Nyangale, S. Farmer, D. Keller, D. Chernoff and G. R. Gibson, Effect of prebiotics on the fecal microbiota of elderly volunteers after dietary supplementation of *Bacillus coagulans* GBI-30, 6086, *Anaerobe*, 2014, **30**, 75–81.
- 22 S. Zhao, X. Peng, Q. Y. Zhou, Y. Y. Huang, X. Rao, J. L. Tu, H. Y. Xiao and D. M. Liu, *Bacillus coagulans* 13002 and fructo-oligosaccharides improve the immunity of mice with immunosuppression induced by cyclophosphamide



- through modulating intestinal-derived and fecal microbiota, *Food Res. Int.*, 2021, **140**, 109793.
- 23 R. K. Kallur, S. Madapati, A. Mathur and S. Bhattacharya, The role of Weizmannia (Bacillus) coagulans LMG S-31876 in treating IBS-diarrhea, *Front. Nutr.*, 2023, **10**, 1310462.
  - 24 E. Cho, J. Y. Kim, B. Cho, J. S. Lee, Y. C. Yoon, Y. C. Shin, H. Kim, S. Gil and S. Kim, Efficacy of fermented grain using Bacillus coagulans in reducing visceral fat among people with obesity: a randomized controlled trial, *Front. Nutr.*, 2023, **10**, 1148512.
  - 25 Z. Z. Alamri, The role of liver in metabolism: an updated review with physiological emphasis, *Int. J. Basic Clin. Pharmacol.*, 2018, **7**, 2271–2276.
  - 26 A. Allameh, R. Niayesh-Mehr, A. Aliarab, G. Sebastiani and K. Pantopoulos, Oxidative Stress in Liver Pathophysiology and Disease, *Antioxidants*, 2023, **12**, 1653.
  - 27 L. X. Li, A. P. Wang, R. Zhang, T. T. Li, J. W. Wang, Y. Q. Bao and W. P. Jia, Decreased urine uric acid excretion is an independent risk factor for chronic kidney disease but not for carotid atherosclerosis in hospital-based patients with type 2 diabetes: a cross-sectional study, *Cardiovasc. Diabetol.*, 2015, **14**, 36.
  - 28 M. Li, X. Wu, Z. Guo, R. Gao, Z. Ni, H. Cui, M. Zong, F. Van Bockstaele and W. Lou, Lactiplantibacillus plantarum enables blood urate control in mice through degradation of nucleosides in gastrointestinal tract, *Microbiome*, 2023, **11**, 153.
  - 29 Y. K. Zhang, J. S. Chen, M. M. Wang, C. Z. Wang, M. X. Wang, Z. Wang, Q. L. Yang, B. Sun, J. Y. Sun, Y. F. Liu and C. Liu, Synthesis and bioactivity evaluation of novel nuciferine derivatives with antihyperuricemia and nephroprotective effects, *Bioorg. Chem.*, 2022, **126**, 105916.
  - 30 M. Q. Zhang, K. X. Sun, X. Guo, Y. Y. Chen, C. Y. Feng, J. S. Chen, J. C. M. Barreira, M. A. Prieto, J. Y. Sun, J. D. Zhang, N. Y. Li and C. Liu, The antihyperuricemia activity of Astragali Radix through regulating the expression of uric acid transporters via PI3K/Akt signalling pathway, *J. Ethnopharmacol.*, 2023, **317**, 116770.
  - 31 J. Tan, L. Wan, X. Chen, X. Li and X. Hao, Conjugated Linoleic Acid Ameliorates High Fructose-Induced Hyperuricemia and Renal Inflammation in Rats via NLRP3 Inflammasome and TLR4 Signaling Pathway, *Mol. Nutr. Food Res.*, 2019, **12**, 1801402.
  - 32 W. Cao, T. Wu, F. Liang, Y. Fang, Y. Cheng, S. Pan and X. Xu, Protective effects of di-caffeoylquinic acids from Artemisia selengensis Turcz leaves against monosodium urate-induced inflammation via the modulation of NLRP3 inflammasome and Nrf2 signaling pathway in THP-1 macrophages, *J. Food Biochem.*, 2022, **46**, e14252.
  - 33 X. Li, Y. Chen, X. Gao, Y. Wu, H. R. El-Seedi, Y. Cao and C. Zhao, Antihyperuricemic Effect of Green Alga Ulva lactuca Ulvan through Regulating Urate Transporters, *J. Agric. Food Chem.*, 2021, **69**, 11225–11235.
  - 34 W. Wu, S. Wang, Q. Liu, T. Shan and Y. Wang, Metformin Protects against LPS-Induced Intestinal Barrier Dysfunction by Activating AMPK Pathway, *Mol. Pharm.*, 2018, **15**, 3272–3284.
  - 35 Y. X. Xu, L. D. Liu, J. Y. Zhu, S. S. Zhu, B. Q. Ye, J. L. Yang, J. Y. Huang, Z. H. Huang, Y. You, W. K. Li, J. L. He, M. Xia and Y. Liu, Alistipes indistinctus-derived hippuric acid promotes intestinal urate excretion to alleviate hyperuricemia, *Cell Host Microbe*, 2024, **32**, 366–381.e369.
  - 36 N. L. Lartey, H. Vargas-Robles, I. M. Guerrero-Fonseca, P. Nava, E. K. Kumatia, A. Ocloo and M. Schnoor, Annickia polycarpa extract attenuates inflammation, neutrophil recruitment, and colon damage during colitis, *Immunol. Lett.*, 2022, **248**, 99–108.
  - 37 C. Feng, W. Zhang, T. Zhang, Q. He, L.-Y. Kwok, Y. Tan and H. Zhang, Heat-Killed Bifidobacterium bifidum B1628 May Alleviate Dextran Sulfate Sodium-Induced Colitis in Mice, and the Anti-Inflammatory Effect Is Associated with Gut Microbiota Modulation, *Nutrients*, 2022, **14**, 5233.
  - 38 X. Shen, A. Xie, Z. Li, C. Jiang, J. Wu, M. Li and X. Yue, Research Progress for Probiotics Regulating Intestinal Flora to Improve Functional Dyspepsia: A Review, *Foods*, 2024, **13**, 151.
  - 39 R. Ranjbar, S. N. Vahdati, S. Tavakoli, R. Khodaie and H. Behboudi, Immunomodulatory roles of microbiota-derived short-chain fatty acids in bacterial infections, *Biomed. Pharmacother.*, 2021, **141**, 111817.
  - 40 K. Ben Salem and A. Ben Abdelaziz, Principal Component Analysis (PCA), *Tunis. Med.*, 2021, **99**, 383–389.
  - 41 J. R. Chen, O. P. Lazarenko, J. Zhang, M. L. Blackburn, M. J. Ronis and T. M. Badger, Diet-derived phenolic acids regulate osteoblast and adipocyte lineage commitment and differentiation in young mice, *J. Bone Miner. Res.*, 2014, **29**, 1043–1053.
  - 42 J. Xia, I. V. Sinelnikov, B. Han and D. S. Wishart, MetaboAnalyst 3.0—making metabolomics more meaningful, *Nucleic Acids Res.*, 2015, **43**, W251–W257.
  - 43 Y. Cheng, D. Sun, B. Zhu, W. Zhou, C. Lv, F. Kou and H. Wei, Integrative Metabolic and Proteomic Profiling of the Brainstem in Spontaneously Hypertensive Rats, *J. Proteome Res.*, 2020, **19**, 4114–4124.
  - 44 X. Shen, C. Wang, N. Liang, Z. Liu, X. Li, Z. J. Zhu, T. R. Merriman, N. Dalbeth, R. Terkeltaub, C. Li and H. Yin, Serum Metabolomics Identifies Dysregulated Pathways and Potential Metabolic Biomarkers for Hyperuricemia and Gout, *Arthritis Rheumatol.*, 2021, **73**, 1738–1748.
  - 45 S. Y. Zhao, Z. L. Liu, Y. S. Shu, M. L. Wang, D. He, Z. Q. Song, H. L. Zeng, Z. C. Ning, C. Lu, A. P. Lu and Y. Y. Liu, Chemotaxonomic Classification Applied to the Identification of Two Closely-Related Citrus TCMS Using UPLC-Q-TOF-MS-Based Metabolomics, *Molecules*, 2017, **22**, 1721.
  - 46 R. Li, Y. Yao, P. Gao and S. Bu, The Therapeutic Efficacy of Curcumin vs. Metformin in Modulating the Gut Microbiota in NAFLD Rats: A Comparative Study, *Front. Microbiol.*, 2020, **11**, 555293.



- 47 O. Popa-Nita, L. Marois, G. Paré and P. H. Naccache, Crystal-induced neutrophil activation: X. Proinflammatory role of the tyrosine kinase Tec, *Arthritis Rheum.*, 2008, **58**, 1866–1876.
- 48 G. K. Ferreira, G. Scaini, M. Carvalho-Silva, L. M. Gomes, L. S. Borges, J. S. Vieira, L. S. Constantino, G. C. Ferreira, P. F. Schuck and E. L. Streck, Effect of L-tyrosine in vitro and in vivo on energy metabolism parameters in brain and liver of young rats, *Neurotoxic. Res.*, 2013, **23**, 327–335.
- 49 J. Feng, C. Ge, W. Li and R. Li, 3-(3-Hydroxyphenyl)propionic acid, a microbial metabolite of quercetin, inhibits monocyte binding to endothelial cells via modulating E-selectin expression, *Fitoterapia*, 2022, **156**, 105071.
- 50 Y. Zhang, W. Yu, D. Han, J. Meng, H. Wang and G. Cao, L-lysine ameliorates sepsis-induced acute lung injury in a lipopolysaccharide-induced mouse model, *Biomed. Pharmacother.*, 2019, **118**, 109307.
- 51 J. W. Ko, H. J. Kwon, C. S. Seo, S. J. Choi, N. R. Shin, S. H. Kim, Y. H. Kim, J. C. Kim, M. S. Kim and I. S. Shin, 4-Hydroxycinnamic acid suppresses airway inflammation and mucus hypersecretion in allergic asthma induced by ovalbumin challenge, *Phytother. Res.*, 2020, **34**, 624–633.
- 52 X. Y. Wang, C. Y. Miao, X. F. Ye, W. Y. Wang, J. B. Zhu, Y. Zhou, Y. Li and J. G. Wang, Dietary cooking oils and cardiometabolic measurements in an elderly Chinese population, *J. Geriatr. Cardiol.*, 2024, **21**, 642–650.
- 53 W. He, A. Henne, M. Lauterbach, E. Geißmar, F. Nikolka, C. Kho, A. Heinz, C. Dostert, M. Grusdat, T. Cordes, J. Härm, O. Goldmann, A. Ewen, C. Verschuere, J. Blay-Cadanet, R. Geffers, H. Garritsen, M. Kneiling, C. K. Holm, C. M. Metallo, E. Medina, Z. Abdullah, E. Latz, D. Brenner and K. Hiller, Mesaconate is synthesized from itaconate and exerts immunomodulatory effects in macrophages, *Nat. Metab.*, 2022, **4**, 524–533.
- 54 M. Ohm, S. Hosseini, N. Lonnemann, W. He, T. More, O. Goldmann, E. Medina, K. Hiller and M. Korte, The potential therapeutic role of itaconate and mesaconate on the detrimental effects of LPS-induced neuroinflammation in the brain, *J. Neuroinflammation*, 2024, **21**, 207.
- 55 C. Proffitt, G. Bidkhor, S. Lee, A. Tebani, A. Mardinoglu, M. Uhlen, D. L. Moyes and S. Shoaie, Genome-scale metabolic modelling of the human gut microbiome reveals changes in the glyoxylate and dicarboxylate metabolism in metabolic disorders, *iScience*, 2022, **25**, 104513.
- 56 R. Bao, Q. Chen, Z. Li, D. Wang, Y. Wu, M. Liu, Y. Zhang and T. Wang, Eurycomanol Alleviates Hyperuricemia by Promoting Uric Acid Excretion and Reducing Purine Synthesis, *Phytomedicine*, 2021, **96**, 153850.
- 57 X. Shi, T. Zhao, E. F. da Silva-Júnior, J. Zhang, S. Xu, S. Gao, X. Liu and P. Zhan, Novel urate transporter 1 (URAT1) inhibitors: a review of recent patent literature (2020-present), *Expert Opin. Ther. Pat.*, 2022, **32**, 1175–1184.
- 58 F. Preitner, O. Bonny, A. Laverrière, S. Rotman, D. Firsov, A. Da Costa, S. Metref and B. Thorens, Glut9 is a major regulator of urate homeostasis and its genetic inactivation induces hyperuricosuria and urate nephropathy, *Proc. Natl. Acad. Sci. U. S. A.*, 2009, **106**, 15501–15506.
- 59 S. Chung and G. H. Kim, Urate Transporters in the Kidney: What Clinicians Need to Know, *Electrolytes Blood Pressure*, 2021, **19**, 1–9.
- 60 L. Zhu, Y. Dong, S. Na, R. Han, C. Wei and G. Chen, Saponins extracted from *Dioscorea collettii* rhizomes regulate the expression of urate transporters in chronic hyperuricemia rats, *Biomed. Pharmacother.*, 2017, **93**, 88–94.
- 61 Y. Toyoda, T. Takada, H. Miyata, H. Matsuo, H. Kassai, K. Nakao, M. Nakatochi, Y. Kawamura, S. Shimizu, N. Shinomiya, K. Ichida, M. Hosoyamada, A. Aiba and H. Suzuki, Identification of GLUT12/SLC2A12 as a urate transporter that regulates the blood urate level in hyperuricemia model mice, *Proc. Natl. Acad. Sci. U. S. A.*, 2020, **117**, 18175–18177.
- 62 Q. Li, H. Lin, Y. Niu, Y. Liu, Z. Wang, L. Song, L. Gao and L. Li, Mangiferin promotes intestinal elimination of uric acid by modulating intestinal transporters, *Eur. J. Pharmacol.*, 2020, **888**, 173490.
- 63 J. Lu, N. Dalbeth, H. Yin, C. Li, T. R. Merriman and W. H. Wei, Mouse models for human hyperuricaemia: a critical review, *Nature reviews, Rheumatology*, 2019, **15**, 413–426.
- 64 Q. Huang, W. Gao, H. Mu, T. Qin, F. Long, L. Ren, H. Tang, J. Liu and M. Zeng, HSP60 Regulates Monosodium Urate Crystal-Induced Inflammation by Activating the TLR4-NF- $\kappa$ B-MyD88 Signaling Pathway and Disrupting Mitochondrial Function, *Oxid. Med. Cell. Longevity*, 2020, **2020**, 8706898.
- 65 C. Y. Hsieh, L. H. Li, Y. K. Rao, T. C. Ju, Y. S. Nai, Y. W. Chen and K. F. Hua, Mechanistic insight into the attenuation of gouty inflammation by Taiwanese green propolis via inhibition of the NLRP3 inflammasome, *J. Cell. Physiol.*, 2019, **234**, 4081–4094.
- 66 E. K. Jo, J. K. Kim, D. M. Shin and C. Sasakawa, Molecular mechanisms regulating NLRP3 inflammasome activation, *Cell. Mol. Immunol.*, 2016, **13**, 148–159.
- 67 A. K. So and F. Martinon, Inflammation in gout: mechanisms and therapeutic targets, *Nature reviews, Rheumatology*, 2017, **13**, 639–647.
- 68 J. Lo, H. E. Wu, C. C. Liu, K. C. Chang, P. Y. Lee, P. L. Liu, S. P. Huang, P. C. Wu, T. C. Lin, Y. H. Lai, Y. C. Chang, Y. R. Chen, S. I. Lee, Y. K. Huang, S. C. Wang and C. Y. Li, Nordalbergin Exerts Anti-Neuroinflammatory Effects by Attenuating MAPK Signaling Pathway, NLRP3 Inflammasome Activation and ROS Production in LPS-Stimulated BV2 Microglia, *Int. J. Mol. Sci.*, 2023, **24**, 7300.
- 69 Q.-Q. Han, Q.-D. Ren, X. Guo, M. A. Farag, Y.-H. Zhang, M.-Q. Zhang, Y.-Y. Chen, S.-T. Sun, J.-Y. Sun, N.-Y. Li and C. Liu, Punicalagin attenuates hyperuricemia via restoring hyperuricemia-induced renal and intestinal dysfunctions, *J. Adv. Res.*, 2025, **69**, 449–461.



- 70 Y. Li, Y. Zhuang, Y. Chen, G. Wang, Z. Tang, Y. Zhong, Y. Zhang, L. Wu, X. Ji, Q. Zhang, B. Pan and Y. Luo, Euphorbia factor L2 alleviated gouty inflammation by specifically suppressing both the priming and activation of NLRP3 inflammasome, *Int. Immunopharmacol.*, 2024, **138**, 112598.
- 71 S. Murakami and H. Motohashi, Roles of Nrf2 in cell proliferation and differentiation, *Free Radical Biol. Med.*, 2015, **88**, 168–178.
- 72 F. Liang, Y. Fang, W. Cao, Z. Zhang, S. Pan and X. Xu, Attenuation of tert-Butyl Hydroperoxide (t-BHP)-Induced Oxidative Damage in HepG2 Cells by Tangeretin: Relevance of the Nrf2-ARE and MAPK Signaling Pathways, *J. Agric. Food Chem.*, 2018, **66**, 6317–6325.
- 73 Y. Zhang, X. Tan, Z. Lin, F. Li, C. Yang, H. Zheng, L. Li, H. Liu and J. Shang, Fucoidan from *Laminaria japonica* Inhibits Expression of GLUT9 and URAT1 via PI3K/Akt, JNK and NF- $\kappa$ B Pathways in Uric Acid-Exposed HK-2 Cells, *Mar. Drugs*, 2021, **19**, 238.
- 74 N. L. Rukavina Mikusic, N. M. Kouyoumdzian and M. R. Choi, Gut microbiota and chronic kidney disease: evidences and mechanisms that mediate a new communication in the gastrointestinal-renal axis, *Pflugers Arch.*, 2020, **472**, 303–320.
- 75 S. Mohammad and C. Thiemermann, Role of Metabolic Endotoxemia in Systemic Inflammation and Potential Interventions, *Front. Immunol.*, 2020, **11**, 594150.
- 76 Q. Lv, D. Xu, X. Zhang, X. Yang, P. Zhao, X. Cui, X. Liu, W. Yang, G. Yang and S. Xing, Association of Hyperuricemia With Immune Disorders and Intestinal Barrier Dysfunction, *Front. Physiol.*, 2020, **11**, 524236.
- 77 J. Cao, T. Wang, Y. Liu, W. Zhou, H. Hao, Q. Liu, B. Yin and H. Yi, *Lactobacillus fermentum* F40–4 ameliorates hyperuricemia by modulating the gut microbiota and alleviating inflammation in mice, *Food Funct.*, 2023, **14**, 3259–3268.
- 78 D. Parada Venegas, M. K. De la Fuente, G. Landskron, M. J. González, R. Quera, G. Dijkstra, H. J. M. Harmsen, K. N. Faber and M. A. Hermoso, Short Chain Fatty Acids (SCFAs)-Mediated Gut Epithelial and Immune Regulation and Its Relevance for Inflammatory Bowel Diseases, *Front. Immunol.*, 2019, **10**, 277.
- 79 Z. Xie, M. Li, M. Qian, Z. Yang and X. Han, Co-Cultures of *Lactobacillus acidophilus* and *Bacillus subtilis* Enhance Mucosal Barrier by Modulating Gut Microbiota-Derived Short-Chain Fatty Acids, *Nutrients*, 2022, **14**, 4475.
- 80 L. Ma, X. Zhao, T. Liu, Y. Wang, J. Wang, L. Kong, Q. Zhao, Y. Chen, L. Chen and H. Zhang, Xuanfei Baidu decoction attenuates intestinal disorders by modulating NF- $\kappa$ B pathway, regulating T cell immunity and improving intestinal flora, *Phytomedicine*, 2022, **101**, 154100.
- 81 K. Cai, X. Y. Cao, F. Chen, Y. Zhu, D. D. Sun, H. B. Cheng, J. A. Duan and S. L. Su, Xianlian Jiedu, Decoction alleviates colorectal cancer by regulating metabolic profiles, intestinal microbiota and metabolites, *Phytomedicine*, 2024, **128**, 155385.
- 82 X. Liu, L. Zhang, D. Wu, J. Liu, G. Li, Z. Zhang and J. Li, Three dietary phenols from pickled radish improve uric acid metabolism disorder in hyperuricemia mice associated with the altered gut microbiota composition, *Food Biosci.*, 2024, **61**, 104802.
- 83 D. S. Wishart, Emerging applications of metabolomics in drug discovery and precision medicine, *Nat. Rev. Drug Discovery*, 2016, **15**, 473–484.
- 84 W. Chen, L. Gong, Z. Guo, W. Wang, H. Zhang, X. Liu, S. Yu, L. Xiong and J. Luo, A novel integrated method for large-scale detection, identification, and quantification of widely targeted metabolites: application in the study of rice metabolomics, *Mol. Plant*, 2013, **6**, 1769–1780.

